ON THE MONOTONICITY OF HIGH ORDER DISCRETE LAPLACIAN *

LOGAN J. CROSS † AND XIANGXIONG ZHANG ‡

Abstract. The monotonicity of discrete Laplacian, i.e., inverse positivity of stiffness matrix, implies discrete maximum principle, which is in general not true for high order schemes on unstructured meshes. But on structured meshes, it is possible to have high order accurate monotone schemes. We first review previously known high order accurate inverse positive schemes, all of which are fourth order accurate with proven monotonicity on uniform meshes. Then we discuss the monotonicity of a fourth order variational difference scheme on quasi-uniform meshes and prove the inverse positivity of a fifth order accurate variational difference scheme on a uniform mesh.

Key words. Inverse positivity, discrete maximum principle, high order accuracy, monotonicity, discrete Laplacian, quasi uniform meshes

AMS subject classifications. 65N30, 65N06, 65N12

1. Introduction.

In many applications, monotone discrete Laplacian operators are desired and useful for ensuring stability such as discrete maximum principle [8] or positivity-preserving of physically positive quantities. Let Δ_h denote the matrix representation of a discrete Laplacian operator, then it is called *monotone* if $(-\Delta_h)^{-1} \geq 0$, i.e., the matrix $(-\Delta_h)^{-1}$ has nonnegative entries. In this paper, all inequalities for matrices are entry-wise inequalities. The simplest second order accurate centered finite difference $u''(x_i) \approx \frac{u(x_{i-1})-2u(x_i)+u(x_{i+1})}{\Delta x^2}$ is monotone because the corresponding matrix $(-\Delta_h)^{-1}$ is an M-matrix thus inverse positive. The most general extension of this result is to state that linear finite element method under a mild mesh constraint forms an M-matrix thus monotone on unstructured triangular meshes [25].

In general, the discrete maximum principle is not true for high order finite element methods on unstructured meshes [13]. On the other hand, there exist a few high order accurate inverse positive schemes on structured meshes. To the best of our knowledge, the followings schemes for solving a Poisson equation are the only ones proven to be monotone beyond the second order accuracy and all of them are fourth order accurate:

1. Fourth order compact finite difference schemes, including the classical 9-point scheme [15, 10, 2] are monotone because the stiffness matrix is an M-matrix.
2. In [3, 5], a fourth order accurate finite difference scheme was constructed. The stiffness matrix is a product of two M-matrices thus monotone.
3. The Lagrangian P^2 finite element method on a regular triangular mesh [24] has a monotone stiffness matrix [20]. On an equilateral triangular mesh, the discrete maximum principle can also be proven [13]. It can be regarded as a finite difference scheme at vertices and edge centers, on which superconvergence of fourth order accuracy holds.
4. Monotonicity was proven in the simplest finite difference implementation of Lagrangian Q^2 finite element scheme on an uniform rectangular mesh for a variable coefficient Poisson equation under suitable mesh constraints [18].

All schemes above can be written in the form $S\mathbf{u} = M\mathbf{f}$ with $S^{-1} \geq 0$ and $M \geq 0$, thus $(-\Delta_h)^{-1} = S^{-1}M \geq 0$, where M denotes the mass matrix. The last two methods

*L. Cross and X. Zhang were supported by the NSF grant DMS-1913120.

†One Allison Way, Indianapolis, IN 46222 (logancross68@gmail.com).

‡Department of Mathematics, Purdue University, 150 N. University Street, West Lafayette, IN 47907-2067 zhan1966@purdue.edu

are variational finite difference schemes, i.e., finite difference schemes constructed from the variational formulation, thus they do not suffer from the drawbacks of the first two conventional finite difference schemes, such as loss of accuracy on quasi-uniform meshes, difficulty with other types of boundary conditions, etc.

For proving inverse positivity, the main viable tool in the literature is to use M-matrices which are inverse positive. All off-diagonal entries of M-matrices must be non-positive. Except the fourth order compact finite difference, all high order accurate schemes induce positive off-diagonal entries, destroying M-matrix structure, which is a major challenge of proving monotonicity. In [5] and [1], and also the appendix in [18], M-matrix factorizations of the form $(-\Delta_h)^{-1} = M_1 M_2$ were shown for special high order schemes but these M-matrix factorizations seem ad hoc and do not apply to other schemes or other equations. In [20], Lorenz proposed some matrix entry-wise inequality for ensuring a matrix to be a product of two M-matrices and applied it to P^2 finite element method on uniform regular triangular meshes. In [18], Lorenz's condition was applied to Q^2 variational difference scheme on uniform meshes.

The main focus of this paper is to discuss Lorenz's condition for a fourth order scheme on nonuniform meshes and higher order accurate schemes. We discuss mesh constraints to preserve monotonicity of Q^2 variational finite difference scheme on a nonuniform mesh. One can of course also discuss P^2 variational difference scheme on a nonuniform regular triangular mesh, but there does not seem to be any advantage of using P^2. The scheme by Q^2 is easier to implement, see Section 7 in [19].

For higher order scheme, it does not seem possible to apply Lorenz's condition directly. Instead, we will demonstrate that Lorenz's condition can be applied to a few auxiliary matrices to establish the monotonicity in Q^3 variational difference scheme. To the best of our knowledge, this is the first time that monotonicity can be proven for a fifth order accurate scheme in two dimensions. For one-dimensional Laplacian, discrete maximum principle was proven for high order finite element methods [22]. We are able to show the fifth order Q^3 variational difference scheme in two dimensions can be factored into a product of four M-matrices, whereas existing M-matrix factorizations for high order schemes involved products of two M-matrices.

The rest of the paper is organized as follows. In Section 2, we briefly review the conventional monotone high order finite difference schemes. In Section 3, we review the fourth order P^2 and Q^2 variational finite difference schemes. In Section 4, we review the Lorenz's condition for proving monotonicity and propose a relaxed version of Lorenz's condition. In Section 5, we discuss the monotonicity of Q^2 variational finite difference scheme on a quasi-uniform mesh. In Section 6, we prove the monotonicity of Q^3 variational finite difference scheme on a uniform mesh. Accuracy tests of these schemes are given in Section 7. Section 8 are concluding remarks.

2. Classical finite difference schemes.

2.1. 9-point scheme. The 9-point scheme was somewhat suggested already in [12] and discussed in details in [10, 15]. It can be extended to higher dimensions [2, 4].

Consider solving the two-dimensional Poisson equations $-u_{xx} - u_{yy} = f$ with homogeneous Dirichlet boundary conditions on a rectangular domain $\Omega = (0,1) \times (0,1)$. Let $u_{i,j}$ denote the numerical solutions at a uniform grid $(x_i, y_j) = (\frac{i}{Nx}, \frac{j}{Ny})$, and $f_{i,j} = f(x_i, y_j)$. For convenience, we introduce two matrices,

$$U = \begin{pmatrix} u_{i-1,j+1} & u_{i,j+1} & u_{i+1,j+1} \\ u_{i-1,j} & u_{i,j} & u_{i+1,j} \\ u_{i-1,j-1} & u_{i,j-1} & u_{i+1,j-1} \end{pmatrix}, \quad F = \begin{pmatrix} f_{i-1,j+1} & f_{i,j+1} & f_{i+1,j+1} \\ f_{i-1,j} & f_{i,j} & f_{i+1,j} \\ f_{i-1,j-1} & f_{i,j-1} & f_{i+1,j-1} \end{pmatrix}.$$

Then the 9-point discrete Laplacian for the Poisson equation at a grid point (x_i, y_j) can be written as

(2.1)
$$\frac{1}{12\Delta x^2}\begin{pmatrix}-1 & 2 & -1\\ -10 & 20 & -10\\ -1 & 2 & -1\end{pmatrix} : U + \frac{1}{12\Delta y^2}\begin{pmatrix}-1 & -10 & -1\\ 2 & 20 & 2\\ -1 & -10 & -1\end{pmatrix} : U = \frac{1}{12}\begin{pmatrix}0 & 1 & 0\\ 1 & 8 & 1\\ 0 & 1 & 0\end{pmatrix} : F.$$

where : denotes the sum of all entry-wise products in two matrices of the same size. Under the assumption $\Delta x = \Delta y = h$, it reduces to the following:

$$\frac{1}{6h^2}\begin{pmatrix}-1 & -4 & -1\\ -4 & 20 & -4\\ -1 & -4 & -1\end{pmatrix} : U = \frac{1}{12}\begin{pmatrix}0 & 1 & 0\\ 1 & 8 & 1\\ 0 & 1 & 0\end{pmatrix} : F. \tag{2.2}$$

The 9-point scheme can also be regarded as a compact finite difference scheme [11]. There can exist a few or many different compact finite difference approximations of the same order [16]. For instance, with the fourth order compact finite difference approximation to Laplacian used in [17], we get the following scheme:

(2.3)
$$\tfrac{1}{12\Delta x^2}\begin{pmatrix}-1 & 2 & -1\\ -10 & 20 & -10\\ -1 & 2 & -1\end{pmatrix} : U + \tfrac{1}{12\Delta y^2}\begin{pmatrix}-1 & -10 & -1\\ 2 & 20 & 2\\ -1 & -10 & -1\end{pmatrix} : U = \tfrac{1}{144}\begin{pmatrix}1 & 10 & 1\\ 10 & 100 & 10\\ 1 & 10 & 1\end{pmatrix} : F.$$

Both schemes (2.1) and (2.3) are fourth order accurate and they have the same stencil and the same stiffness matrix in the left hand side. We have not observed any significant difference in numerical performances between these two schemes.

REMARK 1. *For solving 2D Laplace equation $-\Delta u = 0$ with Dirichlet boundary conditions, the 9-point scheme becomes sixth order accurate [11].*

Nonsingular M-matrices are inverse-positive matrices. There are many equivalent definitions or characterizations of M-matrices, see [21]. The following is a convenient sufficient but not necessary characterization of nonsingular M-matrices [18]:

THEOREM 2.1. *For a real square matrix A with positive diagonal entries and non-positive off-diagonal entries, A is a nonsingular M-matrix if all the row sums of A are non-negative and at least one row sum is positive.*

By condition K_{35} in [21], a sufficient and necessary characterization is,

THEOREM 2.2. *For a real square matrix A with positive diagonal entries and non-positive off-diagonal entries, A is a nonsingular M-matrix if and only if that there exists a positive diagonal matrix D such that AD has all positive row sums.*

REMARK 2. *Non-negative row sum is not a necessary condition for M-matrices. For instance, the following matrix A is an M-matrix by Theorem 2.2:*

$$A = \begin{bmatrix}10 & 0 & 0\\ -10 & 2 & -10\\ 0 & 0 & 10\end{bmatrix}, D = \begin{bmatrix}0.1 & 0 & 0\\ 0 & 2 & 0\\ 0 & 0 & 0.1\end{bmatrix}, AD = \begin{bmatrix}1 & 0 & 0\\ -1 & 4 & -1\\ 0 & 0 & 1\end{bmatrix}.$$

The stiffness matrix in the scheme (2.2) has diagonal entries $\frac{20}{6h^2}$ and offdiagonal entries $-\frac{1}{6h^2}$, $-\frac{4}{6h^2}$ and 0, thus by Theorem 2.1 it is an M-matrix and the scheme is monotone. In order for the stiffness matrix in (2.1) and (2.3) to be an M-matrix, we need all the off-diagonal entries to be nonnegative, which is true under the mesh constraints $\frac{1}{\sqrt{5}} \leq \frac{\Delta x}{\Delta y} \leq \sqrt{5}$.

2.2. The Bramble and Hubbard's scheme. In [5], a fourth order accurate monotone scheme was constructed. Consider solving a one-dimensional problem

$$-u'' = f, \quad x \in [0,1], \quad u(0) = \sigma_0, u(1) = \sigma_1, \tag{2.4}$$

on a uniform grid $x_i = \frac{i}{n+1}$ $(i = 0, 1, \cdots, n+1)$. The scheme can be written as

$$\frac{-\sigma_0 + 2u_1 - u_2}{\Delta x^2} = f_1, \quad \frac{-u_{n-1} + 2u_n - \sigma_1}{\Delta x^2} = f_n$$

$$\frac{\frac{1}{12}u_{i-2} - \frac{4}{3}u_{i-1} + \frac{5}{2}u_i - \frac{4}{3}u_{i+1} + \frac{1}{12}u_{i+2}}{\Delta x^2} = f_i, \quad i = 2, 3, \cdots, n-1.$$

The matrix vector form of the scheme is $\frac{1}{\Delta x^2} H\mathbf{u} = \tilde{\mathbf{f}}$ where

$$H = \begin{pmatrix} 2 & -1 & & & & & \\ -\frac{4}{3} & \frac{5}{2} & -\frac{4}{3} & \frac{1}{12} & & & \\ \frac{1}{12} & -\frac{4}{3} & \frac{5}{2} & -\frac{4}{3} & \frac{1}{12} & & \\ & \ddots & \ddots & \ddots & \ddots & \ddots & \\ & & \frac{1}{12} & -\frac{4}{3} & \frac{5}{2} & -\frac{4}{3} & \frac{1}{12} \\ & & & \frac{1}{12} & -\frac{4}{3} & \frac{5}{2} & -\frac{4}{3} \\ & & & & & -1 & 2 \end{pmatrix}, \mathbf{u} = \begin{pmatrix} u_1 \\ u_2 \\ \\ \vdots \\ \\ u_{n-1} \\ u_n \end{pmatrix}, \tilde{\mathbf{f}} = \begin{pmatrix} f_1 \\ f_2 \\ \\ \vdots \\ \\ f_{n-1} \\ f_n \end{pmatrix} + \begin{pmatrix} \frac{\sigma_0}{\Delta x^2} \\ -\frac{\sigma_0}{12\Delta x^2} \\ \\ \mathbf{0} \\ \\ -\frac{\sigma_1}{12\Delta x^2} \\ \frac{\sigma_1}{\Delta x^2} \end{pmatrix}.$$

For two-dimensional Laplacian, the scheme is defined similarly. In particular, assume $\Delta x = \Delta y = h$ for a square domain, the stiffness matrix can be written as $\frac{1}{h^2}(H \otimes I + I \otimes H)$ where I is the identity matrix and $\otimes$ is the Kronecker product. Its monotonicity was proven in [5].

3. Variational finite difference schemes.

3.1. Finite element method with the simplest quadrature. Consider an elliptic equation on $\Omega = (0,1) \times (0,1)$ with Dirichlet boundary conditions:

$$\mathcal{L}u \equiv -\nabla \cdot (a\nabla u) + cu = f \quad \text{on} \quad \Omega, \quad u = g \quad \text{on} \quad \partial\Omega. \tag{3.1}$$

Assume there is a function $\bar{g} \in H^1(\Omega)$ as an extension of g so that $\bar{g}|_{\partial\Omega} = g$. The variational form of (3.1) is to find $\tilde{u} = u - \bar{g} \in H_0^1(\Omega)$ satisfying

$$\mathcal{A}(\tilde{u}, v) = (f, v) - \mathcal{A}(\bar{g}, v), \quad \forall v \in H_0^1(\Omega), \tag{3.2}$$

where $\mathcal{A}(u,v) = \iint_\Omega a\nabla u \cdot \nabla v dxdy + \iint_\Omega cuvdxdy$, $(f,v) = \iint_\Omega fvdxdy$.

Let h be quadrature point spacing of a regular triangular mesh shown in Figure 1 (or a rectangular mesh shown in Figure 2) and $V_0^h \subseteq H_0^1(\Omega)$ be the continuous finite element space consisting of piecewise P^2 polynomials (or Q^2 polynomials), then the most convenient implementation of finite element method is to use the simple quadrature consisting of vertices and edge centers with equal weights (or 3×3 Gauss-Lobatto quadrature rule) for all the integrals, see Figure 1 for P^2 method (or Figure 2 for Q^2 method). Such a numerical scheme can be defined as: find $u_h \in V_0^h$ satisfying

$$\mathcal{A}_h(u_h, v_h) = \langle f, v_h \rangle_h - \mathcal{A}_h(g_I, v_h), \quad \forall v_h \in V_0^h, \tag{3.3}$$

where $\mathcal{A}_h(u_h, v_h)$ and $\langle f, v_h \rangle_h$ denote using simple quadrature for integrals $\mathcal{A}(u_h, v_h)$ and (f, v_h) respectively, and g_I is the piecewise P^2 (or Q^2) Lagrangian interpolation

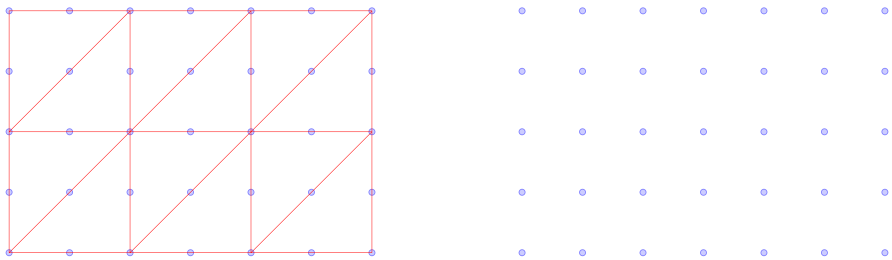

(a) The quadrature points and a finite element mesh for P^2

(b) The corresponding finite difference grid

FIG. 1. *An illustration of Lagrangian P^2 element and the simple quadrature using vertices and edge centers.*

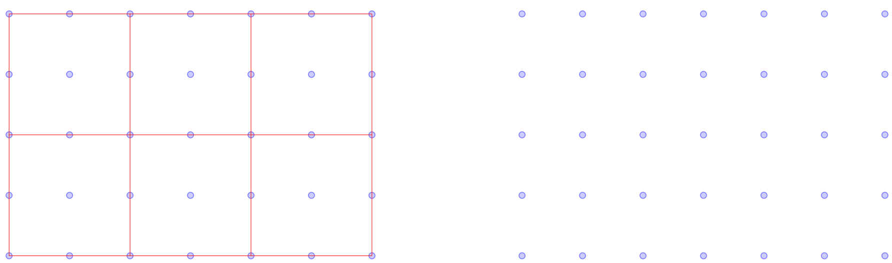

(a) The quadrature points and a finite element mesh

(b) The corresponding finite difference grid

FIG. 2. *An illustration of Lagrangian Q^2 element and the 3×3 Gauss-Lobatto quadrature.*

polynomial at the quadrature points shown in Figure 1 for P^2 method (or Figure 2 for Q^2 method) of the following function:

$$g(x,y) = \begin{cases} 0, & \text{if} \quad (x,y) \in (0,1) \times (0,1), \\ g(x,y), & \text{if} \quad (x,y) \in \partial\Omega. \end{cases}$$

Then $\bar{u}_h = u_h + g_I$ is the numerical solution for the problem (3.1). Notice that (3.3) is not a straightforward approximation to (3.2) since $\bar{g}$ is never used. When the numerical solution is represented by a linear combination of Lagrangian interpolation polynomials at the grid points, it can be rewritten as a finite difference scheme. We also call it a variational difference scheme since it is derived from the variational form.

3.2. The P^2 variational difference scheme derived. For Laplacian $\mathcal{L}u = -\Delta u$, the scheme (3.3) on a uniform regular triangular mesh can be given as [24]:

$$\text{(3.4a)} \qquad \frac{1}{h^2}\begin{pmatrix} 0 & -1 & 0 \\ -1 & 4 & -1 \\ 0 & -1 & 0 \end{pmatrix} : U = f_{i,j}, \quad \text{if } (x_i, y_j) \text{ is an edge center;}$$

$$\text{(3.4b)} \qquad \frac{1}{9h^2}\begin{pmatrix} 1 & -4 & 1 \\ -4 & 12 & -4 \\ 1 & -4 & 1 \end{pmatrix} : U = 0, \quad \text{if } (x_i, y_j) \text{ is a vertex.}$$

Notice that the stiffness matrix is not an M-matrix due to the positive off-diagonal entries in (3.4b) and its inverse positivity was proven in [20].

Since the simple quadrature is exact for integrating only quadratic polynomials on triangles, it is not obvious why the variational difference scheme (3.4) is fourth order accurate. With such a quadrature on two adjacent triangles forming a rectangle in a regular triangular mesh, we obtain a quadrature on the rectangle, see Figure 3. For a reference square $[-1,1]\times[-1,1]$, the quadrature weights are $\frac{2}{3}$ and $\frac{4}{3}$ for an edge center and the cell center respectively.

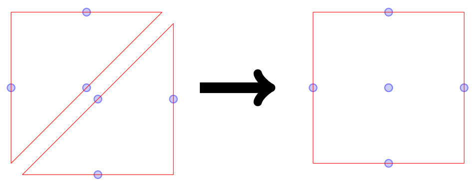

FIG. 3. *The simple quadrature on two triangles give a quadrature on a square.*

LEMMA 3.1. *The quadrature on a square $[-1,1]\times[-1,1]$ using only four edge centers with weight $\frac{2}{3}$ and one cell center with weight $\frac{4}{3}$ is exact for P^3 polynomials.*

Proof. Since the quadrature is exact for integrating P^2 polynomials on either triangle in Figure 3, it suffices to show that it is exact for integrating basis polynomials of degree three, i.e., x^2y, xy^2, x^3 and y^3. It is straightforward to verify that both exact integrals and quadrature of these four polynomials on the square are zero. ∎

Therefore, with Bramble-Hilbert Lemma (see Exercise 3.1.1 and Theorem 4.1.3 in [9]), we can show that the quadrature rule is fourth order accurate if we regard the regular triangular mesh in Figure 3 (a) as a rectangular mesh.

The standard $L^2(\Omega)$-norm estimate for the finite element method with quadrature (3.3) using Lagrangian P^2 elements is third order accurate for smooth exact solutions [9]. On the other hand, superconvergence of function values in finite element method without quadrature can be proven [6, 23], e.g., the errors at vertices and edge centers are fourth order accurate on triangular meshes for function values if using P^2 basis, see also [14]. It can be shown that using such fourth order accurate quadrature will not affect the fourth order superconvergence even for a general variable coefficient elliptic problem, see [19]. Notice that the scheme can also be given on a nonuniform mesh and its fourth order accuracy still holds on a quasi uniform mesh since it is also a finite element method.

3.3. Q^2 variational difference scheme. The scheme (3.3) with Lagrangian Q^2 basis is fourth order accurate [19] and monotone on a uniform mesh under suitable mesh constraints [18]. In the next section, we will discuss its monotonicity for the Laplacian operator on quasi-uniform meshes.

Consider a uniform grid (x_i, y_j) for a rectangular domain $[0,1]\times[0,1]$ where $x_i = ih$, $i = 0,1,\ldots,n+1$ and $y_j = jh$, $j = 0,1,\ldots,n+1$, $h = \frac{1}{n+1}$, where n must be odd. Let u_{ij} denote the numerical solution at (x_i, y_j). Let $\mathbf{u}$ denote an abstract vector consisting of u_{ij} for $i,j = 1,2,\cdots,n$. Let $\bar{\mathbf{u}}$ denote an abstract vector consisting of u_{ij} for $i,j = 0,1,2,\cdots,n,n+1$. Let $\bar{\mathbf{f}}$ denote an abstract vector consisting of f_{ij} for $i,j = 1,2,\cdots,n$ and the boundary condition g at the boundary grid points. Then the matrix vector representation of (3.3) is $S\bar{\mathbf{u}} = M\mathbf{f}$ where S is the stiffness matrix and M is the lumped mass matrix. For convenience, after inverting the mass matrix, with the boundary conditions, the whole scheme can be represented in a matrix vector form $\bar{L}_h\bar{\mathbf{u}} = \bar{\mathbf{f}}$. For Laplacian $\mathcal{L}u = -\Delta u$, $\bar{L}_h\bar{\mathbf{u}} = \bar{\mathbf{f}}$ on a uniform mesh is given as

(3.5)

$$(\bar{L}_h\bar{\mathbf{u}})_{i,j} := \frac{-u_{i-1,j} - u_{i+1,j} + 4u_{i,j} - u_{i,j+1} - u_{i+1,j}}{h^2} = f_{i,j}, \quad \text{if } (x_i, y_j) \text{ is a cell center,}$$

$$(\bar{L}_h\bar{\mathbf{u}})_{i,j} := \frac{-u_{i-1,j} + 2u_{i,j} - u_{i+1,j}}{h^2} + \frac{u_{i,j-2} - 8u_{i,j-1} + 14u_{i,j} - 8u_{i,j+1} + u_{i,j+2}}{4h^2} = f_{i,j},$$
$$\text{if } (x_i, y_j) \text{ is an edge center for an edge parallel to the y-axis,}$$

$$(\bar{L}_h\bar{\mathbf{u}})_{i,j} := \frac{u_{i-2,j} - 8u_{i-1,j} + 14u_{i,j} - 8u_{i+1,j} + u_{i+2,j}}{4h^2} + \frac{-u_{i,j-1} + 2u_{i,j} - u_{i,j+1}}{h^2} = f_{i,j},$$
$$\text{if } (x_i, y_j) \text{ is an edge center for an edge parallel to the x-axis,}$$

$$(\bar{L}_h\bar{\mathbf{u}})_{i,j} := \frac{u_{i-2,j} - 8u_{i-1,j} + 14u_{i,j} - 8u_{i+1,j} + u_{i+2,j}}{4h^2} + \frac{u_{i,j-2} - 8u_{i,j-1} + 14u_{i,j} - 8u_{i,j+1} + u_{i,j+2}}{4h^2} = f_{i,j},$$
$$\text{if } (x_i, y_j) \text{ is a knot,}$$

$$(\bar{L}_h\bar{\mathbf{u}})_{i,j} := u_{i,j} = g_{i,j} \quad \text{if } (x_i, y_j) \text{ is a boundary point.}$$

If ignoring the denominator h^2, then the stencil can be represented as:

$$\text{cell center} \quad \begin{array}{ccc} & -1 & \\ -1 & 4 & -1 \\ & -1 & \end{array} \qquad \text{knots} \quad \begin{array}{ccccc} & & \frac{1}{4} & & \\ & & -2 & & \\ \frac{1}{4} & -2 & 7 & -2 & \frac{1}{4} \\ & & -2 & & \\ & & \frac{1}{4} & & \end{array}$$

$$\text{edge center (edge parallel to } y\text{-axis)} \quad \begin{array}{ccccc} & & -1 & & \\ \frac{1}{4} & -2 & \frac{11}{2} & -2 & \frac{1}{4} \\ & & -1 & & \end{array}$$

$$\text{edge center (edge parallel to } x\text{-axis)} \quad \begin{array}{ccc} & \frac{1}{4} & \\ & -2 & \\ -1 & \frac{11}{2} & -1 \\ & -2 & \\ & \frac{1}{4} & \end{array}$$

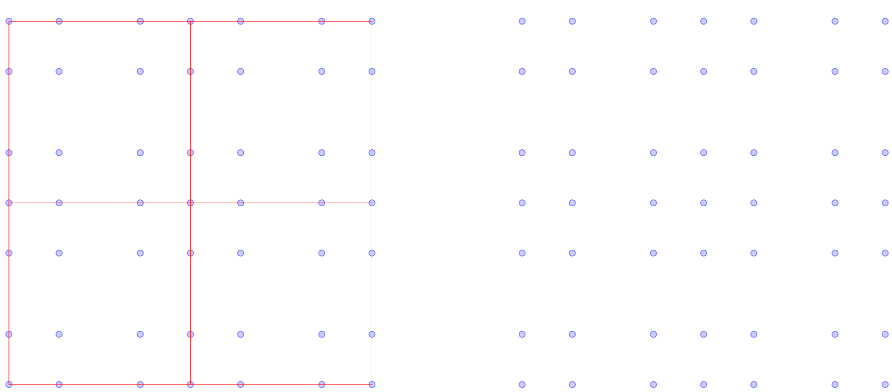

(a) Quadrature points and a finite element mesh.

(b) The corresponding finite difference grid.

FIG. 4. *An illustration of a mesh for Q^3 element and the 4×4 Gauss-Lobatto quadrature.*

3.4. Q^3 variational difference scheme. In (3.3), if using Lagrangian Q^3 basis with 4×4 Gauss-Lobatto quadrature, we get a fifth order accurate scheme [19]. The

FIG. 5. *Three adjacent 1D cells for P^3 elements using 4-point Gauss-Lobatto quadrature.*

4-point Gauss-Lobatto quadrature for the reference interval $[-1, 1]$ has quadrature points $[-1 - \frac{\sqrt{5}}{5}\ \frac{\sqrt{5}}{5}\ 1]$. Thus on an uniform rectangular mesh, the corresponding finite difference grid consisting of quadrature points is not exactly uniform, see Figure 4.

Now consider a uniform mesh for a one-dimensional problem and assume each cell has length h, see Figure 5. There are two quadrature points inside each interval, and we refer to them as the left interior point and the right interior point. The Q^3 variational difference scheme for one-dimension problem (2.4) is given as $\bar{L}_h\bar{\mathbf{u}} = \bar{\mathbf{f}}$:

(3.6)

$$(\bar{L}_h\bar{\mathbf{u}})_i := \frac{4}{h^2}\left[13u_i - \frac{15\sqrt{5}+25}{8}(u_{i-1}+u_{i+1}) + \frac{15\sqrt{5}-25}{8}(u_{i-2}+u_{i+2}) - \frac{1}{4}(u_{i-3}+u_{i+3})\right] = f_i, x_i \text{ is a knot;}$$

$$(\bar{L}_h\bar{\mathbf{u}})_i := \frac{4}{h^2}\left[-\frac{3\sqrt{5}+5}{4}u_{i-1} + 5u_i + \frac{-5}{2}u_{i+1} + \frac{15\sqrt{5}-25}{8}u_{i+2}\right] = f_i, \quad x_i \text{ is the left interior point;}$$

$$(\bar{L}_h\bar{\mathbf{u}})_i := \frac{4}{h^2}\left[\frac{15\sqrt{5}-25}{8}u_{i-2} - \frac{5}{2}u_{i-1} + 5u_i - \frac{3\sqrt{5}+5}{4}u_{i+1}\right] = f_i, \quad \text{if } x_i \text{ is the right interior point.}$$

$$(\bar{L}_h\bar{\mathbf{u}})_0 := u_0 = \sigma_0, \qquad (\bar{L}_h\bar{\mathbf{u}})_{n+1} := u_{n+1} = \sigma_1.$$

The explicit scheme in two dimensions will be given in Section 6.

4. Lorenz's condition for monotonicity.

4.1. Discrete maximum principle.

For a finite difference scheme, assume there are N grid points in the domain Ω and N^∂ boundary grid points on $\partial\Omega$. Define

$$\mathbf{u} = \begin{pmatrix} u_1 & \cdots & u_N \end{pmatrix}^T, \mathbf{u}^\partial = \begin{pmatrix} u_1^\partial & \cdots & u_{N^\partial}^\partial \end{pmatrix}^T, \tilde{\mathbf{u}} = \begin{pmatrix} u_1 & \cdots & u_N & u_1^\partial & \cdots & u_{N^\partial}^\partial \end{pmatrix}^T.$$

A finite difference scheme can be written as

$$\begin{aligned} \mathcal{L}_h(\tilde{\mathbf{u}})_i = \sum_{j=1}^{N} b_{ij}u_j + \sum_{j=1}^{N^\partial} b_{ij}^\partial u_j^\partial =& f_i, \quad 1 \le i \le N, \\ u_i^\partial =& g_i, \quad 1 \le i \le N^\partial. \end{aligned}$$

The matrix form is

$$\tilde{L}_h\tilde{\mathbf{u}} = \tilde{\mathbf{f}}, \tilde{L}_h = \begin{pmatrix} L_h & B^\partial \\ 0 & I \end{pmatrix}, \tilde{\mathbf{u}} = \begin{pmatrix} \mathbf{u} \\ \mathbf{u}^\partial \end{pmatrix}, \tilde{\mathbf{f}} = \begin{pmatrix} \mathbf{f} \\ \mathbf{g} \end{pmatrix}.$$

The discrete maximum principle is

$$\mathcal{L}_h(\tilde{\mathbf{u}})_i \le 0, 1 \le i \le N \Longrightarrow \max_i u_i \le \max\{0, \max_i u_i^\partial\} \tag{4.1}$$

which implies

$$\mathcal{L}_h(\tilde{\mathbf{u}})_i = 0, 1 \le i \le N \Longrightarrow |u_i| \le \max_i |u_i^\partial|.$$

The following result was proven in [8]:

THEOREM 4.1. *A finite difference operator $\mathcal{L}_h$ satisfies the discrete maximum principle (4.1) if $\tilde{L}_h^{-1} \ge 0$ and all row sums of $\tilde{L}_h$ are non-negative.*

With the same $\bar{L}_h$ as defined in the previous section, it suffices to have $\bar{L}_h^{-1} \geq 0$, see [18]:

THEOREM 4.2. *If $\bar{L}_h^{-1} \geq 0$, then $\tilde{L}_h^{-1} \geq 0$ thus $L_h^{-1} \geq 0$. Moreover, if row sums of $\bar{L}_h$ are non-negative, then the finite difference operator $\mathcal{L}_h$ satisfies the discrete maximum principle.*

Let $\mathbf{1}$ be an abstract vector of the same shape as $\bar{\mathbf{u}}$ with all ones. For the Q^2 or Q^3 variational difference scheme, we have that $(\bar{L}_h\mathbf{1})_{i,j} = 1$ if $(x_i, y_j) \in \partial\Omega$ and $(\bar{L}_h\mathbf{1})_{i,j} = 0$ if $(x_i, y_j) \in \Omega$, which implies the row sums of $\bar{L}_h$ are non-negative. Thus from now on, we only need to discuss the monotonicity of the matrix $\bar{L}_h$.

4.2. Lorenz's sufficient condition for monotonicity.

DEFINITION 1. *Let $\mathcal{N} = \{1, 2, \dots, n\}$. For $\mathcal{N}_1, \mathcal{N}_2 \subset \mathcal{N}$, we say a matrix A of size $n \times n$ connects $\mathcal{N}_1$ with $\mathcal{N}_2$ if*

$$\forall i_0 \in \mathcal{N}_1, \exists i_r \in \mathcal{N}_2, \exists i_1, \dots, i_{r-1} \in \mathcal{N} \quad s.t. \quad a_{i_{k-1}i_k} \neq 0, \quad k = 1, \cdots, r. \tag{4.2}$$

If perceiving A as a directed graph adjacency matrix of vertices labeled by $\mathcal{N}$, then (4.2) simply means that there exists a directed path from any vertex in $\mathcal{N}_1$ to at least one vertex in $\mathcal{N}_2$. In particular, if $\mathcal{N}_1 = \emptyset$, then any matrix A connects $\mathcal{N}_1$ with $\mathcal{N}_2$.

Given a square matrix A and a column vector $\mathbf{x}$, we define

$$\mathcal{N}^0(A\mathbf{x}) = \{i : (A\mathbf{x})_i = 0\}, \quad \mathcal{N}^+(A\mathbf{x}) = \{i : (A\mathbf{x})_i > 0\}.$$

Given a matrix $A = [a_{ij}] \in \mathbb{R}^{n\times n}$, define its diagonal, off-diagonal, positive and negative off-diagonal parts as $n \times n$ matrices A_d, A_a, A_a^+, A_a^-:

$$(A_d)_{ij} = \begin{cases} a_{ii}, & \text{if} \quad i = j \\ 0, & \text{if} \quad i \neq j \end{cases}, \quad A_a = A - A_d,$$

$$(A_a^+)_{ij} = \begin{cases} a_{ij}, & \text{if} \quad a_{ij} > 0, \quad i \neq j \\ 0, & \text{otherwise.} \end{cases}, \quad A_a^- = A_a - A_a^+.$$

The following two results were proven in [20]. See also [18] for a detailed proof.

THEOREM 4.3. *If $A \leq M_1 M_2 \cdots M_k L$ where $M_1, \cdots, M_k$ are nonsingular M-matrices and $L_a \leq 0$, and there exists a nonzero vector $\mathbf{e} \geq 0$ such that one of the matrices $M_1, \cdots, M_k, L$ connects $\mathcal{N}^0(A\mathbf{e})$ with $\mathcal{N}^+(A\mathbf{e})$. Then $M_k^{-1}M_{k-1}^{-1} \cdots M_1^{-1}A$ is an M-matrix, thus A is a product of $k+1$ nonsingular M-matrices and $A^{-1} \geq 0$.*

THEOREM 4.4 (Lorenz's condition). *If A_a^- has a decomposition: $A_a^- = A^z + A^s = (a_{ij}^z) + (a_{ij}^s)$ with $A^s \leq 0$ and $A^z \leq 0$, such that*

$$A_d + A^z \text{ is a nonsingular M-matrix,} \tag{4.3a}$$

$$A_a^+ \leq A^z A_d^{-1} A^s \text{ or equivalently } \forall a_{ij} > 0 \text{ with } i \neq j, a_{ij} \leq \sum_{k=1}^n a_{ik}^z a_{kk}^{-1} a_{kj}^s, \tag{4.3b}$$

$$\exists \mathbf{e} \in \mathbb{R}^n \setminus \{\mathbf{0}\}, \mathbf{e} \geq 0 \text{ with } A\mathbf{e} \geq 0 \text{ s.t. } A^z \text{ or } A^s \text{ connects } \mathcal{N}^0(A\mathbf{e}) \text{ with } \mathcal{N}^+(A\mathbf{e}). \tag{4.3c}$$

Then A is a product of two nonsingular M-matrices thus $A^{-1} \geq 0$.

COROLLARY 4.5. *The matrix L in Theorem 4.3 must be an M-matrix.*

Proof. Let $M^{-1} = M_k^{-1} M_{k-1}^{-1} ... M_1^{-1}$, following the proof of Theorem 7 in [18], then $M^{-1}A\mathbf{e} \geq cA\mathbf{e}$ for some positive number c. Then $A\mathbf{e} \geq 0 \Rightarrow M^{-1}A\mathbf{e} \geq 0$. Now since $\mathbf{e} \geq 0$, $M^{-1}A \leq L \Rightarrow 0 \leq (L - M^{-1}A)\mathbf{e} \Rightarrow M^{-1}A\mathbf{e} \leq L\mathbf{e}$ thus $L\mathbf{e} \geq 0$.

Assume L connects $\mathcal{N}^0(A\mathbf{e})$ with $\mathcal{N}^+(A\mathbf{e})$. Since $M^{-1}A\mathbf{e} \leq L\mathbf{e}$, $\mathcal{N}^0(L\mathbf{e}) \subseteq \mathcal{N}^0(A\mathbf{e})$ and $\mathcal{N}^+(A\mathbf{e}) \subseteq \mathcal{N}^+(L\mathbf{e})$, so L also connects $\mathcal{N}^0(L\mathbf{e})$ with $\mathcal{N}^+(L\mathbf{e})$.

Assume M_i connects $\mathcal{N}^0(A\mathbf{e})$ with $\mathcal{N}^+(A\mathbf{e})$, following the proof of Theorem 7 in [18], we have $M^{-1}A\mathbf{e} > 0$. Now L trivially connects $\mathcal{N}^0(L\mathbf{e})$ with $\mathcal{N}^+(L\mathbf{e})$ since $L\mathbf{e} \geq M^{-1}A\mathbf{e} \Rightarrow L\mathbf{e} > 0$ and $\mathcal{N}^0(L\mathbf{e}) = \emptyset$.

Then Theorem 6 in [18] applies to show L is an M-matrix. ∎

In practice, the condition (4.3c) can be difficult to verify. For variational difference schemes, the vector $\mathbf{e}$ can be taken as $\mathbf{1}$ consisting of all ones, then the condition (4.3c) can be simplified. The following theorem was proven in [18].

THEOREM 4.6. *Let A denote the matrix representation of the variational difference scheme (3.3) with Q^2 basis solving $-\nabla \cdot (a\nabla)u + cu = f$. Assume A_a^- has a decomposition $A_a^- = A^z + A^s$ with $A^s \leq 0$ and $A^z \leq 0$. Then $A^{-1} \geq 0$ if the following are satisfied:*

1. *$(A_d + A^z)\mathbf{1} \neq \mathbf{0}$ and $(A_d + A^z)\mathbf{1} \geq 0$;*
2. *$A_a^+ \leq A^z A_d^{-1} A^s$;*
3. *For $c(x, y) \geq 0$, either A^z or A^s has the same sparsity pattern as A_a^-. If $c(x, y) > 0$, then this condition can be removed.*

4.3. A relaxed Lorenz's condition. In practice, both (4.3a) and (4.3b) impose mesh constraints for the Q^2 variational difference scheme on non-uniform meshes. The condition (4.3a) can be relaxed as the following:

THEOREM 4.7 (A relaxed Lorenz's condition). *If A_a^- has a decomposition: $A_a^- = A^z + A^s = (a_{ij}^z) + (a_{ij}^s)$ with $A^s \leq 0$ and $A^z \leq 0$, and there exists a diagonal matrix $A_{d^*} \geq A_d$ such that*

(4.4a)
$$A_d^* + A^z \text{ is a nonsingular M-matrix,}$$

(4.4b)
$$A_a^+ \leq A^z A_{d^*}^{-1} A^s,$$

(4.4c)
$$\exists \mathbf{e} \in \mathbb{R}^n \setminus \{\mathbf{0}\}, \mathbf{e} \geq 0 \text{ with } A\mathbf{e} \geq 0 \text{ s.t. } A^z \text{ or } A^s \text{ connects } \mathcal{N}^0(A\mathbf{e}) \text{ with } \mathcal{N}^+(A\mathbf{e}).$$

Then A is a product of two nonsingular M-matrices thus $A^{-1} \geq 0$.

Proof. It is straightforward that $A = A_d + A_a^+ + A^z + A^s \leq A_{d^*} + A^z + A^s + A^z A_{d^*}^{-1} A^s = (A_{d^*} + A^z)(I + A_{d^*}^{-1} A^s)$. By (4.4c), either $A_{d^*} + A^z$ or $I + A_{d^*}^{-1} A^s$ connects $\mathcal{N}^0(A\mathbf{e})$ with $\mathcal{N}^+(A\mathbf{e})$. By applying Theorem 4.3 for the case $k = 1$, $M_1 = A_{d^*} + A^z$ and $L = I + A_{d^*}^{-1} A^s$, we get $A^{-1} \geq 0$. ∎

REMARK 3. *Since $A_d \leq A_{d^*}$, only (4.4a) is more relaxed than (4.3a), and (4.4b) is more stringent than (4.3b). However, we will show in next section that it is possible to construct A_{d^*} such that (4.3b) and (4.4b) impose identical mesh constraints.*

With Theorem 2.1, combining Theorem 4.7 and Theorem 4.6, we have:

THEOREM 4.8. *Let A denote the matrix representation of the variational difference scheme (3.3) with Q^2 basis solving $-\nabla \cdot (a\nabla)u + cu = f$. Assume A_a^- has a* *decomposition $A_a^- = A^z + A^s$ with $A^s \leq 0$ and $A^z \leq 0$ and there exists a diagonal matrix $A_{d^*} \geq A_d$. Then $A^{-1} \geq 0$ if the following are satisfied:*

1. *$(A_{d^*} + A^z)\mathbf{1} \neq \mathbf{0}$ and $(A_{d^*} + A^z)\mathbf{1} \geq 0$;*
2. *$A_a^+ \leq A^z A_{d^*}^{-1} A^s$;*
3. *For $c(x, y) \geq 0$, either A^z or A^s has the same sparsity pattern as A_a^-. If $c(x, y) > 0$, then this condition can be removed.*

5. Monotonicity of Q^2 variational difference scheme on quasi-uniform meshes. The discussion in this section can be easily extended to more general cases such as $\mathcal{L}u = -\Delta u + cu$ and Neumann boundary conditions. For simplicity, we only discuss the Laplacian case $\mathcal{L}u = -\Delta u$ and Dirichlet boundary conditions.

Consider a grid (x_i, y_j) $(i, j = 0, 1, \ldots, n+1)$ for a rectangular domain $[0, 1]\times[0, 1]$ where n must be odd and $i, j = 0, n+1$ correspond to boundary points. Let u_{ij} denote the numerical solution at (x_i, y_j). Let $\bar{\mathbf{u}}$ denote an abstract vector consisting of u_{ij} for $i, j = 0, 1, 2, \cdots, n, n + 1$. Let $\bar{\mathbf{f}}$ denote an abstract vector consisting of f_{ij} for $i, j = 1, 2, \cdots, n$ and the boundary condition g at the boundary grid points. Then the matrix vector representation of (3.3) with Q^2 basis is $\bar{L}_h \bar{\mathbf{u}} = \bar{\mathbf{f}}$.

The focus of this section is to show $\bar{L}_h^{-1} \geq 0$ under suitable mesh constraints for quasi-uniform meshes. Moreover, it is straightforward to verify that $(\bar{L}_h \mathbf{1})_{i,j} = 0$ for interior points (x_i, y_j) and $(\bar{L}_h \mathbf{1})_{i,j} = 1$ for boundary points (x_i, y_j). Thus by Section 4.1, the scheme also satisfies the discrete maximum principle.

For simplicity, in the rest of this section we use A to denote the matrix $\bar{L}_h$ and let $\mathcal{A}$ be the linear operator corresponding to the matrix A. For convenience, we can also regard the abstract vector $\bar{\mathbf{u}}$ as a matrix of size $(n+2)\times(n+2)$. Then by our notation, the mapping $\mathcal{A} : \mathbb{R}^{(n+2)\times(n+2)} \to \mathbb{R}^{(n+2)\times(n+2)}$ is given as $\mathcal{A}(\bar{\mathbf{u}})_{i,j} := (\bar{L}_h \bar{\mathbf{u}})_{i,j}$.

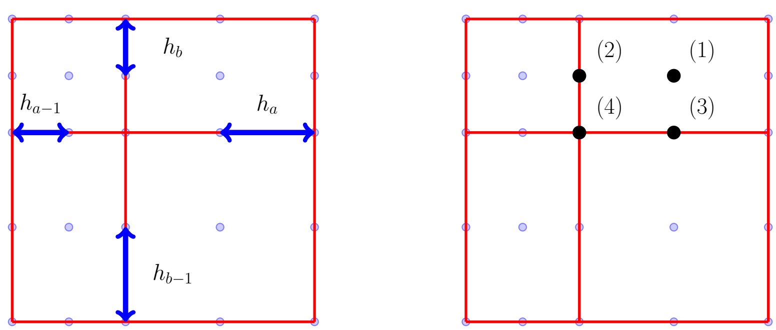

(a) Mesh length definitions for four adjacent Q^2 elements.

(b) The four distinct point types.

FIG. 6. *A non-uniform mesh for Q^2 variational difference scheme. Each edge in a cell has length $2h$.*

5.1. The scheme in two dimensions. For boundary points $(x_i, y_j) \in \partial\Omega$, the scheme is $\mathcal{A}(\bar{\mathbf{u}})_{i,j} := u_{i,j} = g_{i,j}$. The scheme for interior grid points $(x_i, y_j) \in \Omega$ on a non-uniform mesh can be given on four distinct types of points shown in Figure 6 (b). For simplicity, from now on, we will use *edge center (2)* to denote an interior edge center for an edge parallel to the y-axis, and *edge center (3)* to denote an interior edge center for an edge parallel to the x-axis. The scheme at an interior grid point is given as $\mathcal{A}(\bar{\mathbf{u}})_{i,j} = f_{i,j}$ with

(5.1)
$$
\begin{aligned}
\mathcal{A}(\bar{\mathbf{u}})_{i,j} :=& \frac{2h_a^2+2h_b^2}{h_a^2h_b^2}u_{i,j} - \left(\frac{1}{h_a^2}u_{i+1,j} + \frac{1}{h_a^2}u_{i-1,j} + \frac{1}{h_b^2}u_{i,j+1} + \frac{1}{h_b^2}u_{i,j-1}\right) \\
& \text{if } (x_i, y_j) \text{ is a cell center;} \\
\mathcal{A}(\bar{\mathbf{u}})_{i,j} :=& \frac{7h_b^2+4h_ah_{a-1}}{2h_ah_{a-1}h_b^2}u_{i,j} - \frac{4}{h_a(h_a+h_{a-1})}u_{i+1,j} - \frac{4}{h_{a-1}(h_a+h_{a-1})}u_{i-1,j} \\
& - \frac{1}{h_b^2}u_{i,j+1} - \frac{1}{h_b^2}u_{i,j-1} + \frac{1}{2h_a(h_a+h_{a-1})}u_{i+2,j} + \frac{1}{2h_{a-1}(h_a+h_{a-1})}u_{i-2,j}, \\
& \text{if } (x_i, y_j) \text{ is edge center (2);} \\
\mathcal{A}(\bar{\mathbf{u}})_{i,j} :=& \frac{7h_a^2+4h_bh_{b-1}}{2h_bh_{b-1}h_a^2}u_{i,j} - \frac{4}{h_b(h_b+h_{b-1})}u_{i,j+1} - \frac{4}{h_{b-1}(h_b+h_{b-1})}u_{i,j-1} \\
& - \frac{1}{h_a^2}u_{i+1,j} - \frac{1}{h_a^2}u_{i-1,j} + \frac{1}{2h_b(h_b+h_{b-1})}u_{i,j+2} + \frac{1}{2h_{b-1}(h_b+h_{b-1})}u_{i,j-2}, \\
& \text{if } (x_i, y_j) \text{ is edge center (3);} \\
\mathcal{A}(\bar{\mathbf{u}})_{i,j} :=& \frac{7h_ah_{a-1}+7h_bh_{b-1}}{2h_ah_{a-1}h_bh_{b-1}}u_{i,j} - \left[\frac{4}{h_a(h_a+h_{a-1})}u_{i+1,j} + \frac{4}{h_{a-1}(h_a+h_{a-1})}u_{i-1,j}\right. \\
& \left. + \frac{4}{h_b(h_b+h_{b-1})}u_{i,j+1} + \frac{4}{h_{b-1}(h_b+h_{b-1})}u_{i,j-1}\right] + \frac{1}{2h_a(h_a+h_{a-1})}u_{i+2,j} \\
& + \frac{1}{2h_{a-1}(h_a+h_{a-1})}u_{i-2,j} + \frac{1}{2h_b(h_b+h_{b-1})}u_{i,j+2} + \frac{1}{2h_{b-1}(h_b+h_{b-1})}u_{i,j-2}, \\
& \text{if } (x_i, y_j) \text{ is an interior knot.}
\end{aligned}
$$

For a uniform mesh $h_a = h_{a-1} = h_b = h_{b-1} = h$, the scheme reduces to (3.5).

5.2. The Decomposition of A_a^-. Next, by the same notations defined in Section 4.2, we will decompose the matrix $A = A_d + A_a^- + A_a^+$ and $A_a^- = A^z + A^s$ to verify Theorem 4.6. We will use $\mathcal{A}_a^-$, $\mathcal{A}_a^+$, $\mathcal{A}^z$ and $\mathcal{A}^s$ to denote linear operators for corresponding matrices. First, for the diagonal part we have

$$
\begin{aligned}
&\mathcal{A}_d(\bar{\mathbf{u}})_{i,j} = u_{i,j}, \quad \text{if } (x_i, y_j) \text{ is a boundary point;} \\
&\mathcal{A}_d(\bar{\mathbf{u}})_{i,j} = \frac{2h_a^2+2h_b^2}{h_a^2h_b^2}u_{i,j}, \quad \text{if } (x_i, y_j) \text{ is a cell center;} \\
&\mathcal{A}_d(\bar{\mathbf{u}})_{i,j} = \frac{7h_b^2+4h_ah_{a-1}}{2h_ah_{a-1}h_b^2}u_{i,j}, \quad \text{if } (x_i, y_j) \text{ is edge center (2);} \\
&\mathcal{A}_d(\bar{\mathbf{u}})_{i,j} = \frac{7h_a^2+4h_bh_{b-1}}{2h_bh_{b-1}h_a^2}u_{i,j}, \quad \text{if } (x_i, y_j) \text{ is edge center (3);} \\
&\mathcal{A}_d(\bar{\mathbf{u}})_{i,j} = \frac{7h_bh_{b-1}+7h_ah_{a-1}}{2h_ah_{a-1}h_bh_{b-1}}u_{i,j}, \quad \text{if } (x_i, y_j) \text{ is an interior knot.}
\end{aligned}
$$

Notice that for a boundary point $(x_i, y_j) \in \partial\Omega$ we have $\mathcal{A}(\bar{\mathbf{u}})_{i,j} = \mathcal{A}_d(\bar{\mathbf{u}})_{i,j} = u_{i,j}$, thus for off-diagonal parts, we only need to look at the interior grid points. For positive off-diagonal entries, we have

$$
\begin{aligned}
\mathcal{A}_a^+(\bar{\mathbf{u}})_{i,j} =& 0, \quad \text{if } (x_i, y_j) \text{ is a cell center;}\\
\mathcal{A}_a^+(\bar{\mathbf{u}})_{i,j} =& \frac{1}{2h_a(h_a+h_{a-1})}u_{i+2,j} + \frac{1}{2h_{a-1}(h_a+h_{a-1})}u_{i-2,j}, \quad \text{edge center (2);}\\
\mathcal{A}_a^+(\bar{\mathbf{u}})_{i,j} =& \frac{1}{2h_b(h_b+h_{b-1})}u_{i,j+2} + \frac{1}{2h_{b-1}(h_b+h_{b-1})}u_{i,j-2}, \quad \text{edge center (3);}\\
\mathcal{A}_a^+(\bar{\mathbf{u}})_{i,j} =& \frac{1}{2h_a(h_a+h_{a-1})}u_{i+2,j} + \frac{1}{2h_{a-1}(h_a+h_{a-1})}u_{i-2,j} + \frac{1}{2h_b(h_b+h_{b-1})}u_{i,j+2}\\
&+ \frac{1}{2h_{b-1}(h_b+h_{b-1})}u_{i,j-2}, \quad \text{if } (x_i, y_j) \text{ is an interior knot.}
\end{aligned}
$$

Then we perform a decomposition $A_a^- = A^z + A^s$, which depends on two constants $0 < \epsilon_1 \leq 1$ and $0 < \epsilon_2 \leq 1$.

$$
\begin{aligned}
\mathcal{A}^z(\bar{\mathbf{u}})_{i,j} =& -\epsilon_1\left(\frac{1}{h_a^2}u_{i+1,j} + \frac{1}{h_a^2}u_{i-1,j} + \frac{1}{h_b^2}u_{i,j+1} + \frac{1}{h_b^2}u_{i,j-1}\right), \quad \text{if } (x_i, y_j) \text{ is a cell center;}\\
\mathcal{A}^z(\bar{\mathbf{u}})_{i,j} =& -\epsilon_1\left(\frac{1}{h_b^2}u_{i,j+1} + \frac{1}{h_b^2}u_{i,j-1}\right) - \epsilon_2\left[\frac{4}{h_a(h_a+h_{a-1})}u_{i+1,j} + \frac{4}{h_{a-1}(h_a+h_{a-1})}u_{i-1,j}\right],\\
&\quad \text{if } (x_i, y_j) \text{ is edge center (2);}\\
\mathcal{A}^z(\bar{\mathbf{u}})_{i,j} =& -\epsilon_1\left(\frac{1}{h_a^2}u_{i+1,j} + \frac{1}{h_a^2}u_{i-1,j}\right) - \epsilon_2\left[\frac{4}{h_b(h_b+h_{b-1})}u_{i,j+1} + \frac{4}{h_{b-1}(h_b+h_{b-1})}u_{i,j-1}\right],\\
&\quad \text{if } (x_i, y_j) \text{ is edge center (3);}\\
\mathcal{A}^z(\bar{\mathbf{u}})_{i,j} =& -\epsilon_2\left[\frac{4}{h_a(h_a+h_{a-1})}u_{i+1,j} + \frac{4}{h_{a-1}(h_a+h_{a-1})}u_{i-1,j}\right.\\
&\left. + \frac{4}{h_b(h_b+h_{b-1})}u_{i,j+1} + \frac{4}{h_{b-1}(h_b+h_{b-1})}u_{i,j-1}\right], \quad \text{if } (x_i, y_j) \text{ is an interior knot.} \quad \blacksquare
\end{aligned}
$$

Notice that A^z defined above has exactly the same sparsity pattern as A_a^- for $0 < \epsilon_1 \leq 1$ and $0 < \epsilon_2 \leq 1$. Let $A^s = A_a^- - A^z$ then $A^s \leq 0$.

5.3. Mesh constraints for $A^z A_d^{-1} A^s \geq A_a^+$. In order to verify $A^z A_d^{-1} A^s \geq A_a^+$, we only need to discuss nonzero entries in the output of $\mathcal{A}_a^+(\bar{\mathbf{u}})$ since $A^z A_d^{-1} A^s \geq 0$.

First consider the case that (x_i, y_j) is an interior knot. Figure 7 (a) shows the positive coefficients in the output of $\mathcal{A}_a^+(\bar{\mathbf{u}})_{ij}$ at a knot (x_i, y_j). Figure 7 (b) shows the stencil of $\mathcal{A}^z(\bar{\mathbf{u}})_{ij}$. Thus $\mathcal{A}^z(\bar{\mathbf{u}})$ acting as an operator on $[\mathcal{A}_d^{-1}\mathcal{A}^s](\bar{\mathbf{u}})$ at a knot is:

$$
\begin{aligned}
[\mathcal{A}^z\mathcal{A}_d^{-1}\mathcal{A}^s](\bar{\mathbf{u}})_{i,j} = -4\epsilon_2 &\left[\frac{1}{h_a(h_{a-1}+h_a)}[\mathcal{A}_d^{-1}\mathcal{A}^s](\bar{\mathbf{u}})_{i+1,j} + \frac{1}{h_{a-1}(h_{a-1}+h_a)}[\mathcal{A}_d^{-1}\mathcal{A}^s](\bar{\mathbf{u}})_{i-1,j}\right.\\
&\left. + \frac{1}{h_b(h_{b-1}+h_b)}[\mathcal{A}_d^{-1}\mathcal{A}^s](\bar{\mathbf{u}})_{i,j+1} + \frac{1}{h_{b-1}(h_{b-1}+h_b)}[\mathcal{A}_d^{-1}\mathcal{A}^s](\bar{\mathbf{u}})_{i,j-1}\right].
\end{aligned}
$$

In the expression above, the output of the operator $\mathcal{A}^z(\bar{\mathbf{u}})_{ij}$ are at interior edge centers as shown in Figure 7 (b). Hence $[\mathcal{A}_d^{-1}\mathcal{A}^s]$ will act on these edge centers with the mesh lengths corresponding to Figure 6. Carefully considering the mesh lengths

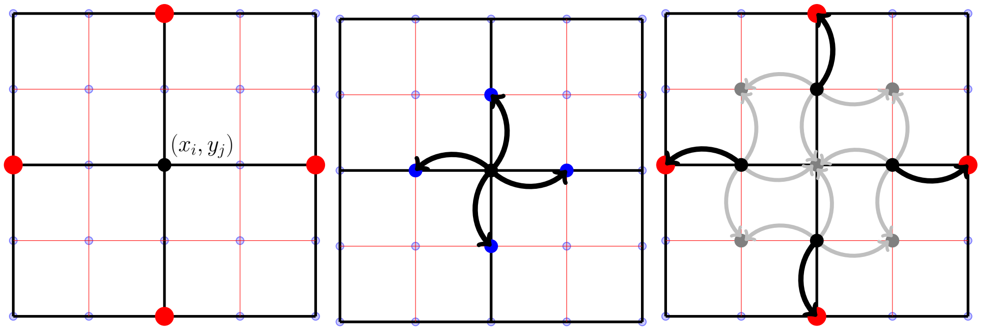

(a) Four red dots denote nonzero entry locations in $\mathcal{A}_a^+(\bar{\mathbf{u}})_{i,j}$

(b) Stencil of $\mathcal{A}^z(\bar{\mathbf{u}})_{i,j}$.

(c) Stencil of $\mathcal{A}^z\mathcal{A}_d^{-1}\mathcal{A}^s(\bar{\mathbf{u}})_{i,j}$.

FIG. 7. *Stencil of operators at an interior knot (x_i, y_j). The four red dots are the locations/entries where $\mathcal{A}_a^+(\bar{\mathbf{u}})_{i,j}$ are nonzero. Gray nodes in (c) represent positive entries that can be discarded for the purposes of verifying* (4.4b). *The mesh is illustrated as a uniform one only for simplicity.*

and operations of $\mathcal{A}_d^{-1}$ at these points gives:

$$[\mathcal{A}^z\mathcal{A}_d^{-1}\mathcal{A}^s](\bar{\mathbf{u}})_{i,j} = -4\epsilon_2\left[\frac{1}{h_a(h_{a-1}+h_a)}\frac{2h_bh_{b-1}h_a^2}{7h_a^2+4h_bh_{b-1}}\mathcal{A}^s(\bar{\mathbf{u}})_{i+1,j}\right.$$
$$+\frac{1}{h_{a-1}(h_{a-1}+h_a)}\frac{2h_bh_{b-1}h_{a-1}^2}{7h_{a-1}^2+4h_bh_{b-1}}\mathcal{A}^s(\bar{\mathbf{u}})_{i-1,j}+\frac{1}{h_b(h_{b-1}+h_b)}\frac{2h_ah_{a-1}h_b^2}{7h_b^2+4h_ah_{a-1}}\mathcal{A}^s(\bar{\mathbf{u}})_{i,j+1}$$
$$\left.+\frac{1}{h_{b-1}(h_{b-1}+h_b)}\frac{2h_ah_{a-1}h_{b-1}^2}{7h_{b-1}^2+4h_ah_{a-1}}\mathcal{A}^s(\bar{\mathbf{u}})_{i,j-1}\right], \quad \text{if } (x_i, y_j) \text{ is an interior knot.}$$

Next consider the effect of $\mathcal{A}^s(\bar{\mathbf{u}})$ operator which has the same sparsity pattern as $\mathcal{A}^z(\bar{\mathbf{u}})$. Figure 7 (c) shows the stencil of $[\mathcal{A}^z\mathcal{A}_d^{-1}\mathcal{A}^s](\bar{\mathbf{u}})_{i,j}$ for an interior knot. Recall that $A^z \leq 0$, $A^s \leq 0$, and $A_d^{-1} \geq 0$, thus we have $A^zA_d^{-1}A^s \geq 0$. So we only need to compare the outputs of $[\mathcal{A}^z\mathcal{A}_d^{-1}\mathcal{A}^s](\bar{\mathbf{u}})_{i,j}$ and $\mathcal{A}_a^+(\bar{\mathbf{u}})_{i,j}$ at nonzero entries of $\mathcal{A}_a^+(\bar{\mathbf{u}})_{i,j}$, i.e., the four red dots in Figure 7 (a) and Figure 7 (c).

Thus we only need coefficients of $u_{i+2,j}, u_{i-2,j}, u_{i,j+2}$, and $u_{i,j-2}$ in the final expression of $[\mathcal{A}^z\mathcal{A}_d^{-1}\mathcal{A}^s](\mathbf{u})_{i,j}$, which are found to be

$$u_{i+2,j}: \quad 4\epsilon_2(1-\epsilon_1)\tfrac{1}{h_a(h_{a-1}+h_a)}\tfrac{2h_bh_{b-1}h_a^2}{7h_a^2+4h_bh_{b-1}}\tfrac{1}{h_a^2}$$
$$u_{i-2,j}: \quad 4\epsilon_2(1-\epsilon_1)\tfrac{1}{h_{a-1}(h_{a-1}+h_a)}\tfrac{2h_bh_{b-1}h_{a-1}^2}{7h_{a-1}^2+4h_bh_{b-1}}\tfrac{1}{h_{a-1}^2}$$
$$u_{i,j+2}: \quad 4\epsilon_2(1-\epsilon_1)\tfrac{1}{h_b(h_{b-1}+h_b)}\tfrac{2h_ah_{a-1}h_b^2}{7h_b^2+4h_ah_{a-1}}\tfrac{1}{h_b^2}$$
$$u_{i,j-2}: \quad 4\epsilon_2(1-\epsilon_1)\tfrac{1}{h_{b-1}(h_{b-1}+h_b)}\tfrac{2h_ah_{a-1}h_{b-1}^2}{7h_{b-1}^2+4h_ah_{a-1}}\tfrac{1}{h_{b-1}^2}$$

In order to maintain $A_a^+ \leq A^zA_d^{-1}A^s$, by comparing to the coefficients of $u_{i+2,j}$ for $\mathcal{A}_a^+(\bar{\mathbf{u}})$, we obtain a mesh constraint $4\epsilon_2(1-\epsilon_1)\frac{2h_bh_{b-1}}{7h_a^2+4h_bh_{b-1}} \geq \frac{1}{2}$. Similar constraints are obtained by comparing other coefficients at $u_{i,j\mp2}$ and $u_{i-2,j}$. Define

$$\ell(\epsilon_1, \epsilon_2) = 4\epsilon_2(1-\epsilon_1).$$

Then the following constraints are sufficient for $\mathcal{A}_a^+(\bar{\mathbf{u}})$ to be controlled by $\mathcal{A}^z\mathcal{A}_d^{-1}\mathcal{A}^s(\bar{\mathbf{u}})$ at an interior knot:

$$\text{(5.2a)} \qquad h_ah_{a-1} \geq \frac{7}{4\ell-4}\max\{h_b^2, h_{b-1}^2\}, \quad h_bh_{b-1} \geq \frac{7}{4\ell-4}\max\{h_a^2, h_{a-1}^2\}.$$

Second, we need to discuss the case when (x_i, y_j) is an interior edge center. Without loss of generality, assume (x_i, y_j) is an interior edge center of an edge parallel to the y-axis. Then similar to the interior knot case, the output coefficients of $[\mathcal{A}^z\mathcal{A}_d^{-1}\mathcal{A}^s](\bar{\mathbf{u}})_{i,j}$ at the relevant non-zero entries of $\mathcal{A}_a^+(\bar{\mathbf{u}})_{i,j}$ are:

$$u_{i+2,j}: \quad 4\epsilon_2(1-\epsilon_1)\tfrac{1}{h_a(h_{a-1}+h_a)}\tfrac{h_a^2h_b^2}{2h_a^2+2h_b^2}\tfrac{1}{h_a^2}$$

$$u_{i-2,j}: \quad 4\epsilon_2(1-\epsilon_1)\tfrac{1}{h_{a-1}(h_{a-1}+h_a)}\tfrac{h_{a-1}^2h_b^2}{2h_{a-1}^2+2h_b^2}\tfrac{1}{h_{a-1}^2}$$

By comparing with coefficients of $\mathcal{A}_a^+(\bar{\mathbf{u}})_{i,j}$, we get $\frac{h_b^2}{h_a^2+h_b^2} \geq \frac{1}{\ell}$, $\quad \frac{h_b^2}{h_{a-1}^2+h_b^2} \geq \frac{1}{\ell}$. To ensure $\mathcal{A}_a^+(\bar{\mathbf{u}})$ is controlled by $\mathcal{A}^z\mathcal{A}_d^{-1}\mathcal{A}^s(\bar{\mathbf{u}})$ at edge centers, it suffices to have:
(5.2b)

$$min\{h_a,h_{a-1}\} \geq \sqrt{\frac{1}{\ell-1}}max\{h_b,h_{b-1}\}, \quad min\{h_b,h_{b-1}\} \geq \sqrt{\frac{1}{\ell-1}}max\{h_a,h_{a-1}\}.$$

Note that $\mathcal{A}_a^+(\bar{\mathbf{u}})_{i,j} = 0$ if (x_i, y_j) is a cell center. Since $\mathcal{A}^z\mathcal{A}_d^{-1}\mathcal{A}^s(\bar{\mathbf{u}}) \geq 0$, there is no mesh constraint to enforce the inequality at cell centers.

5.4. Mesh constraints for $A_d + A^z$ being an M-matrix. Let $\mathcal{B} = \mathcal{A}_d + \mathcal{A}^z$. Then $\mathcal{B}(\mathbf{1})_{i,j} = 1$ for a boundary point (x_i, y_j). For interior points, we have:

$$\mathcal{B}(\mathbf{1})_{i,j} = -\epsilon_1\left(\frac{1}{h_a^2}+\frac{1}{h_a^2}+\frac{1}{h_b^2}+\frac{1}{h_b^2}\right)+\frac{2h_a^2+2h_b^2}{h_a^2h_b^2} = (1-\epsilon_1)\frac{2h_a^2+2h_b^2}{h_a^2h_b^2}, \quad \text{cell center;}$$

$$\begin{aligned}\mathcal{B}(\mathbf{1})_{i,j} &= -\epsilon_1\left(\frac{1}{h_b^2}+\frac{1}{h_b^2}\right)-\epsilon_2\left[\frac{4}{h_a(h_a+h_{a-1})}+\frac{4}{h_{a-1}(h_a+h_{a-1})}\right]+\frac{7h_b^2+4h_ah_{a-1}}{2h_ah_{a-1}h_b^2}\\ &= (1-\epsilon_1)\frac{2}{h_b^2}+(1-\frac{8}{7}\epsilon_2)\frac{7}{2h_ah_{a-1}}, \quad \text{edge center (2);}\end{aligned}$$

$$\begin{aligned}\mathcal{B}(\mathbf{1})_{i,j} &= -\epsilon_1\left(\frac{1}{h_a^2}+\frac{1}{h_a^2}\right)-\epsilon_2\left[\frac{4}{h_b(h_b+h_{b-1})}+\frac{4}{h_{b-1}(h_b+h_{b-1})}\right]+\frac{7h_a^2+4h_bh_{b-1}}{2h_bh_{b-1}h_a^2}\\ &= (1-\epsilon_1)\frac{2}{h_a^2}+(1-\frac{8}{7}\epsilon_2)\frac{7}{2h_bh_{b-1}}, \quad \text{edge center (3);}\end{aligned}$$

$$\begin{aligned}\mathcal{B}(\mathbf{1})_{i,j} &= -\epsilon_2\left[\frac{4}{h_a(h_a+h_{a-1})}+\frac{4}{h_{a-1}(h_a+h_{a-1})}+\frac{4}{h_b(h_b+h_{b-1})}+\frac{4}{h_{b-1}(h_b+h_{b-1})}\right]\\ &\quad+\frac{7h_bh_{b-1}+7h_ah_{a-1}}{2h_ah_{a-1}h_bh_{b-1}} = (1-\frac{8}{7}\epsilon_2)\frac{7h_bh_{b-1}+7h_ah_{a-1}}{2h_ah_{a-1}h_bh_{b-1}}, \quad \text{interior knot.} \quad \blacksquare\end{aligned}$$

Notice that larger values of ℓ give better mesh constraints in (5.2). And we have $\sup_{0<\epsilon_1,\epsilon_2\leq 1}\ell(\epsilon_1,\epsilon_2) = \sup_{0<\epsilon_1,\epsilon_2\leq 1} 4\epsilon_2(1-\epsilon_1) = 4$. In order to apply Theorem 2.1 for $A_d + A^z$ be an M-matrix, we need $[\mathcal{A}_d + \mathcal{A}^z](\mathbf{1}) \geq 0$. This is true if and only if $\epsilon_1 \leq 1$ and $\epsilon_2 \leq \frac{7}{8}$, which only give $\sup_{0<\epsilon_1\leq 1, 0<\epsilon_2\leq\frac{7}{8}}\ell(\epsilon_1,\epsilon_2) = 3.5$.

5.5. Improved mesh constraints by the relaxed Lorenz's condition. To get a better mesh constraint, the constraint on ϵ_2 can be relaxed so that the value of $\ell(\epsilon_1, \epsilon_2)$ can be improved. One observation from Section 5.3 is that the value of $\mathcal{A}_d(\bar{\mathbf{u}})_{i,j}$ for (x_i, y_j) being a knot is not used for verifying $A_a^+ \leq A^zA_d^{-1}A^s$ (for both interior knots and edge centers). To this end, we define a new diagonal matrix A_{d^*}, which is different from A_d only at the interior knots.

$$\begin{aligned}
&\mathcal{A}_{d^*}(\bar{\mathbf{u}})_{i,j} = u_{i,j} = \mathcal{A}_d(\bar{\mathbf{u}})_{i,j}, \quad \text{if } (x_i, y_j) \text{ is a boundary point;}\\
&\mathcal{A}_{d^*}(\bar{\mathbf{u}})_{i,j} = \frac{2h_a^2 + 2h_b^2}{h_a^2 h_b^2} u_{i,j} = \mathcal{A}_d(\bar{\mathbf{u}})_{i,j}, \quad \text{if } (x_i, y_j) \text{ is a cell center;}\\
&\mathcal{A}_{d^*}(\bar{\mathbf{u}})_{i,j} = \frac{7h_b^2 + 4h_a h_{a-1}}{2h_a h_{a-1} h_b^2} u_{i,j} = \mathcal{A}_d(\bar{\mathbf{u}})_{i,j}, \quad \text{edge center (2);}\\
&\mathcal{A}_{d^*}(\bar{\mathbf{u}})_{i,j} = \frac{7h_a^2 + 4h_b h_{b-1}}{2h_b h_{b-1} h_a^2} u_{i,j} = \mathcal{A}_d(\bar{\mathbf{u}})_{i,j}, \quad \text{edge center (3);}\\
&\mathcal{A}_{d^*}(\bar{\mathbf{u}})_{i,j} = \frac{8h_b h_{b-1} + 8h_a h_{a-1}}{2h_a h_{a-1} h_b h_{b-1}} u_{i,j} \neq \mathcal{A}_d(\bar{\mathbf{u}})_{i,j}, \quad \text{if } (x_i, y_j) \text{ is an interior knot.}
\end{aligned}$$

Since the values of $\mathcal{A}_d(\bar{\mathbf{u}})_{i,j}$ for (x_i, y_j) being a knot is not involved in Section 5.3, the same discussion in Section 5.3 also holds for verifying $A_a^+ \leq A^z A_{d^*}^{-1} A^s$. Namely, under mesh constraints (5.2), we also have $A_a^+ \leq A^z A_{d^*}^{-1} A^s$.

Let $B^* = A_{d^*} + A^z$, then the row sums of B^* are:

$$\begin{aligned}
&\mathcal{B}^*(\mathbf{1})_{i,j} = 1, \quad \text{if } (x_i, y_j) \text{ is a boundary point;}\\
&\mathcal{B}^*(\mathbf{1})_{i,j} = -\epsilon_1 \left(\frac{1}{h_a^2} + \frac{1}{h_a^2} + \frac{1}{h_b^2} + \frac{1}{h_b^2} \right) + \frac{2h_a^2 + 2h_b^2}{h_a^2 h_b^2} = (1 - \epsilon_1) \frac{2h_a^2 + 2h_b^2}{h_a^2 h_b^2}, \text{cell center;}\\
&\mathcal{B}^*(\mathbf{1})_{i,j} = -\epsilon_1 \left(\frac{1}{h_b^2} + \frac{1}{h_b^2} \right) - \epsilon_2 \left[\frac{4}{h_a(h_a + h_{a-1})} + \frac{4}{h_{a-1}(h_a + h_{a-1})} \right] + \frac{7h_b^2 + 4h_a h_{a-1}}{2h_a h_{a-1} h_b^2}\\
&\qquad\qquad = (1 - \epsilon_1) \frac{2}{h_b^2} + (1 - \frac{8}{7}\epsilon_2) \frac{7}{2h_a h_{a-1}}, \quad \text{edge center (2);}\\
&\mathcal{B}^*(\mathbf{1})_{i,j} = -\epsilon_1 \left(\frac{1}{h_a^2} + \frac{1}{h_a^2} \right) - \epsilon_2 \left[\frac{4}{h_b(h_b + h_{b-1})} + \frac{4}{h_{b-1}(h_b + h_{b-1})} \right] + \frac{7h_a^2 + 4h_b h_{b-1}}{2h_b h_{b-1} h_a^2}\\
&\qquad\qquad = (1 - \epsilon_1) \frac{2}{h_a^2} + (1 - \frac{8}{7}\epsilon_2) \frac{7}{2h_b h_{b-1}}, \quad \text{edge center (3);}\\
&\mathcal{B}^*(\mathbf{1})_{i,j} = -\epsilon_2 \left[\frac{4}{h_a(h_a + h_{a-1})} + \frac{4}{h_{a-1}(h_a + h_{a-1})} + \frac{4}{h_b(h_b + h_{b-1})} + \frac{4}{h_{b-1}(h_b + h_{b-1})} \right]\\
&\qquad\qquad + \frac{8h_b h_{b-1} + 8h_a h_{a-1}}{2h_a h_{a-1} h_b h_{b-1}} = (1 - \epsilon_2) \frac{8h_b h_{b-1} + 8h_a h_{a-1}}{2h_a h_{a-1} h_b h_{b-1}}, \quad \text{interior knot.}
\end{aligned}$$

$\blacksquare$

Now $[\mathcal{A}_{d^*} + \mathcal{A}^z](\mathbf{1})_{i,j} \geq 0$ at cell centers and knots is true if and only if $\epsilon_1 \leq 1$ and $\epsilon_2 \leq 1$.

Next, we will show that the mesh constraints (5.2) with $0 < \epsilon_1 \leq \frac{1}{2}$ and $\epsilon_2 = 1$ are sufficient to ensure $[\mathcal{A}_{d^*} + \mathcal{A}^z](\mathbf{1})_{i,j} \geq 0$ at edge centers. We have $0 < \epsilon_1 \leq \frac{1}{2}, \epsilon_2 = 1 \implies 2 \leq \ell < 4 \implies \frac{7}{4\ell - 4} \geq \frac{1}{\ell}$. The mesh constraints (5.2) imply that $h_a h_{a-1} \geq \frac{7}{4\ell-4} h_b^2 \geq \frac{1}{\ell} h_b^2$, thus

$$(1 - \epsilon_1) \frac{2}{h_b^2} + (1 - \frac{8}{7}\epsilon_2) \frac{7}{2h_a h_{a-1}} = (1 - \epsilon_1) \frac{2}{h_b^2} - \frac{1}{2} \frac{1}{h_a h_{a-1}} = \frac{1}{2} \left[\frac{\ell}{h_b^2} - \frac{1}{h_a h_{a-1}} \right] \geq 0.$$

Similarly, $(1 - \epsilon_1)\frac{2}{h_a^2} + (1 - \frac{8}{7}\epsilon_2)\frac{7}{2h_b h_{b-1}} \geq 0$ also holds.

Therefore, for constants $0 < \epsilon_1 \leq \frac{1}{2}$ and $\epsilon_2 = 1$, we have $[\mathcal{A}_{d^*} + \mathcal{A}^z](\mathbf{1}) \geq \mathbf{0}$. In particular, we have a larger ℓ compared to constraints from $\mathbf{A}_d$.

5.6. The main result. We have shown that for two constants $0 < \epsilon_1 \le \frac{1}{2}$ and $\epsilon_2 = 1$, under mesh constraints (5.2), the matrices A_{d^*}, A^z, A^s constructed above satisfy $(A_{d^*} + A^z)\mathbf{1} \ge \mathbf{0}$ and $A_a^+ \le A^z A_{d^*}^{-1} A^s$.

For any fixed $\epsilon_1 > 0$ and $\epsilon_2 = 1$, A^z also has the same sparsity pattern as A. Thus if ℓ in (5.2) is replaced by $\sup_{0<\epsilon_1\le\frac{1}{2},\epsilon_2=1} \ell(\epsilon_1, \epsilon_2) = 4$, Theorem 4.8 still applies to conclude that $A^{-1} \ge 0$.

THEOREM 5.1. *The Q^2 variational difference scheme (5.1) has a monotone matrix $\bar{L}_h$ thus satisfies discrete maximum principle under the following mesh constraints:*

$$\begin{aligned} h_a h_{a-1} \ge \frac{7}{12} max\{h_b^2, h_{b-1}^2\}, \quad h_b h_{b-1} \ge \frac{7}{12} max\{h_a^2, h_{a-1}^2\}, \\ min\{h_a, h_{a-1}\} \ge \sqrt{\frac{1}{3}} max\{h_b, h_{b-1}\}, \quad min\{h_b, h_{b-1}\} \ge \sqrt{\frac{1}{3}} max\{h_a, h_{a-1}, \} \end{aligned} \tag{5.3}$$

where h_a, h_{a-1} are mesh sizes for x-axis and h_b, h_{b-1} are mesh sizes for y-variable in four adjacent rectangular cells as shown in Figure 6.

REMARK 4. *The following global constraint is sufficient to ensure (5.3):*

$$\frac{25}{32} \le \frac{h_m}{h_n} \le \frac{32}{25}, \tag{5.4}$$

where h_m and h_n are any two grid spacings in a non-uniform grid generated from a non-uniform rectangular mesh for Q^2 elements.

REMARK 5. *For Q^1 finite element method solving $-\Delta u = f$ to satisfy discrete maximum principle on non-uniform rectangular meshes [7], the mesh constraints are*

$$h_a h_{a-1} \ge \frac{1}{2} max\{h_b^2, h_{b-1}^2\} \quad h_b h_{b-1} \ge \frac{1}{2} max\{h_a^2, h_{a-1}^2\}. \tag{5.5}$$

5.7. Necessity of Mesh Constraints. Even though the mesh constraints derived above are only sufficient conditions, in practice a mesh constraint is still necessary for the inverse positivity to hold. Consider a non-uniform Q^2 mesh with 5×5 cells on the domain $[0,1] \times [0,1]$, which has a 9×9 grid for the interior of the domain. Let the mesh on both axes be the same and let the four outer-most cells for each dimension be identical with length $2h$. Then the middle cell has size $2h' \times 2h'$ with $h' = \frac{1}{2} - 2h$. Let the ratio h'/h increase gradually from $h'/h = 1$ (a uniform mesh) until the minimum value of the inverse of the matrix becomes negative. Increasing by values of 0.05, we obtain the first negative entry of $\bar{L}_h^{-1}$ at $h'/h = 5.35$ with $h = 0.0535$ and $h' = 0.2861$ shown in Figure 8 (a). Figure 8 (b) shows how the minimum entry of $\bar{L}_h^{-1}$ decreases as h'/h increases.

6. Monotonicity of Q^3 variational difference scheme on a uniform mesh. Even though Lorenz's condition can be nicely verified for the Q^2 scheme, it is very difficult to apply Lorenz's condition to higher order schemes due to their much more complicated structure. In particular, even for Q^3 scheme, simple decomposition of $A_a^- = A^z + A^s$ such that $A_a^+ \le A^z A_d^{-1} A^s$ is difficult to show. Instead, we propose to apply Lorenz's theorems to a few simpler intermediate matrices. To be specific, let $A = A_3$ be the matrix representation of the scheme, and let $A_0 = M_1$ be an M-matrix. Then we construct matrices A_i and L_i such that

$$A_1 \le A_0 L_0, \quad A_2 \le A_1 L_1, \quad A_3 \le A_2 L_2,$$

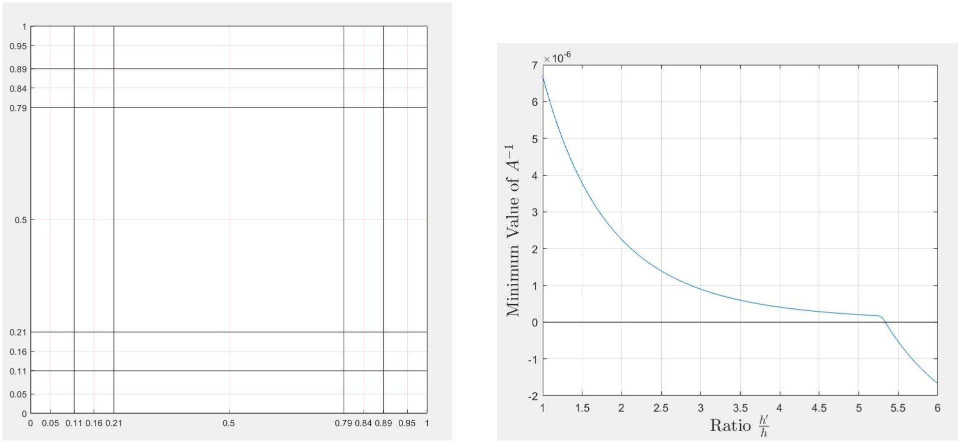

(a) A non-uniform mesh with 5×5 cells on which the $C^0 - Q^2$ scheme is not inverse positive. The minimum value of $\bar{L}_h^{-1}$ is $-6.14E-8$.

(b) A plot of the minimum value of $\bar{L}_h^{-1}$ as h'/h increases.

FIG. 8. *Necessity of mesh constraints for inverse positivity $\bar{L}_h^{-1} \geq 0$ where $\bar{L}_h$ is the matrix in Q^2 variational difference scheme on non-uniform meshes.*

with the constraints that $A_i\mathbf{1} \geq 0$ and $A_0 = M_1$ connects $\mathcal{N}^0(A_i\mathbf{1})$ with $\mathcal{N}^+(A_i\mathbf{1})$ for all A_i. By Theorem 4.3, then we have

$$A_1 \leq A_0L_0 = M_1L_0 \Rightarrow A_1 = M_1M_2 \Rightarrow A_2 \leq M_1M_2L_1 \Rightarrow A_2 = M_1M_2M_3$$

$$\Rightarrow A_3 \leq M_1M_2M_3L_2 \Rightarrow A = A_3 = M_1M_2M_3M_4.$$

The matrices A_i and L_i satisfying constraints above are not unique.

6.1. One-dimensional scheme. We first demonstrate the main idea for the one-dimensional case, for which we only need to construct matrices such that $A_1 \leq A_0L_0, A \leq A_1L_1$.

Let $\bar{L}_h$ denote the coefficient matrix in (3.6), then consider $A = \frac{h^2}{4}\bar{L}_h$. For convenience, we will perceive the matrix A as a linear operator $\mathcal{A}$. Notice that the coefficients for two interior points are symmetric in (3.6), thus we will only show stencil for the left interior point for simplicity:

$$\mathcal{A} \text{ at boundary point } x_0 \text{ or } x_{n+1} : \mathbf{\frac{h^2}{4}}$$

$$\mathcal{A} \text{ at knot} : -\frac{1}{4} \quad \frac{15\sqrt{5}-25}{8} \quad \frac{-15\sqrt{5}-25}{8} \quad \mathbf{13} \quad \frac{-15\sqrt{5}-25}{8} \quad \frac{15\sqrt{5}-25}{8} \quad -\frac{1}{4}$$

$$\mathcal{A} \text{ at interior point} : \quad \frac{-3\sqrt{5}-5}{4} \quad \mathbf{5} \quad -\frac{5}{2} \quad \frac{3\sqrt{5}-5}{4},$$

where bolded entries indicate the coefficient for the operator output location x_i.

For all the matrices defined below, they will have symmetric structure at two interior points, thus for simplicity we will only show the stencil of the corresponding linear operators for the left interior point. We first define three matrices A_1, A_0, and

Z_0.

$$
\begin{aligned}
\mathcal{A}_1 \text{ at boundary}: &\quad \frac{\mathbf{h^2}}{\mathbf{4}} \\
\mathcal{A}_1 \text{ at knot}: &\quad 0 \quad \frac{15\sqrt{5}-25}{8} \quad -7 \quad \mathbf{13} \quad -7 \quad \frac{15\sqrt{5}-25}{8} \quad 0 \\
\mathcal{A}_1 \text{ at interior point}: &\quad -\frac{1}{2} \quad \mathbf{4.8} \quad -2 \quad 0 \\
\mathcal{A}_0 \text{ at boundary}: &\quad \frac{\mathbf{h^2}}{\mathbf{4}} \\
\mathcal{A}_0 \text{ at knot}: &\quad 0 \quad 0 \quad -7 \quad \mathbf{15} \quad -7 \quad 0 \quad 0 \\
\mathcal{A}_0 \text{ at interior point}: &\quad -\frac{1}{2} \quad \mathbf{4.8} \quad -\frac{1}{2} \quad 0 \\
\mathcal{Z}_0 \text{ at boundary}: &\quad \mathbf{0} \\
\mathcal{Z}_0 \text{ at knot}: &\quad 0 \quad 0 \quad 0 \quad \mathbf{0} \quad 0 \quad 0 \quad 0 \\
\mathcal{Z}_0 \text{ at interior point}: &\quad 0 \quad \mathbf{0} \quad -2+\frac{1}{2} \quad 0
\end{aligned}
$$

Then we define $L_0 = I + (A_0)_d^{-1} Z_0$ where I is the identity matrix and $(A_0)_d$ denotes the diagonal part of A_0. By considering composition of two operators $\mathcal{A}_0$ and $\mathcal{L}_0$, we get the matrix product $A_0 L_0$. Due to the definition of Z_0, $\mathcal{A}_0\mathcal{L}_0$ still has the same stencil as above:

$$
\begin{aligned}
\mathcal{A}_0\mathcal{L}_0 \text{ at boundary}: &\quad \frac{\mathbf{h^2}}{\mathbf{4}} \\
\mathcal{A}_0\mathcal{L}_0 \text{ at knot}: &\quad 0 \quad \frac{35}{16} \quad -7 \quad \mathbf{15} \quad -7 \quad \frac{35}{16} \quad 0 \\
\mathcal{A}_0\mathcal{L}_0 \text{ at interior point}: &\quad -\frac{1}{2} \quad \mathbf{4.8} + \frac{\mathbf{5}}{\mathbf{32}} \quad -2 \quad 0
\end{aligned}
$$

It is straightforward to see $A_1 \le A_0 L_0$. By Theorem 2.1, A_0 is an M-matrix, thus we set $M_1 = A_0$. Also it is easy to see that $\mathcal{A}_1(\mathbf{1}) > 0$ thus $\mathcal{N}^0(A_1\mathbf{1})$ is an empty set. So A_0 trivially connects $\mathcal{N}^0(A_1\mathbf{1})$ with $\mathcal{N}^+(A_1\mathbf{1})$. By Theorem 4.3, we have $A_1 \le A_0 L_0 = M_1 L_0 \Rightarrow A_1 = M_1 M_2$ where M_2 is an M-matrix.

Let $(A_1)_d$ denote the diagonal part of A_1. Then define $L_1 = I + (A_1)_d^{-1} Z_1$ using the following Z_1:

$$
\begin{aligned}
\mathcal{Z}_1 \text{ at boundary}: &\quad \mathbf{0} \\
\mathcal{Z}_1 \text{ at knot}: &\quad 0 \quad 0 \quad 0 \quad \mathbf{0} \quad 0 \quad 0 \quad 0 \\
\mathcal{Z}_1 \text{ at interior point}: &\quad -\frac{11}{10} \quad \mathbf{0} \quad -\frac{1}{2} \quad 0
\end{aligned}
$$

And the matrix $A_1 L_1$ still have the same stencil and symmetry:

$$
\begin{aligned}
&\mathcal{A}_1\mathcal{L}_1 \text{ at boundary}: \quad \frac{\mathbf{h^2}}{\mathbf{4}} \\
&\mathcal{A}_1\mathcal{L}_1 \text{ at knot}: \quad \frac{-165\sqrt{5}+275}{384} \quad \frac{15\sqrt{5}-25}{8}+\frac{35}{48} \quad -7+\frac{-75\sqrt{5}+125}{384} \quad \mathbf{13}+\mathbf{2}\left(\frac{\mathbf{77}}{\mathbf{48}}\right) \quad -7+\frac{-75\sqrt{5}+125}{384} \quad \frac{15\sqrt{5}-25}{8}+\frac{35}{48} \quad \frac{-165\sqrt{5}+275}{384} \\
&\mathcal{A}_1\mathcal{L}_1 \text{ at interior point}: \quad -\frac{8}{5} \quad \mathbf{4.8} + \frac{\mathbf{5}}{\mathbf{24}} \quad -\frac{5}{2} \quad \frac{11}{24}
\end{aligned}
$$

A direct comparison verifies that $A \le A_1 L_1 = M_1 M_2 L_1$. Also it is easy to see that $\mathcal{A}(\mathbf{1})_i = 0$ if x_i is not a boundary point. The operator $\mathcal{A}_0$ has a three-point stencil at interior grid points, thus the directed graph defined by the adjacency matrix A_0 has a directed path starting from any interior grid point to any other point, see Figure 9. So $M_1 = A_0$ connects $\mathcal{N}^0(A\mathbf{1})$ with $\mathcal{N}^+(A\mathbf{1})$. By Theorem 4.3, we have $A \leq A_1 L_1 = M_1 M_2 L_1 \Rightarrow A = M_1 M_2 M_3$ where M_3 is an M-matrix. Therefore, $A^{-1} = M_3^{-1} M_2^{-1} M_1^{-1} \geq 0$.

FIG. 9. *The directed graph defined by matrix M_1 for the finite difference grid shown in Figure 5.*

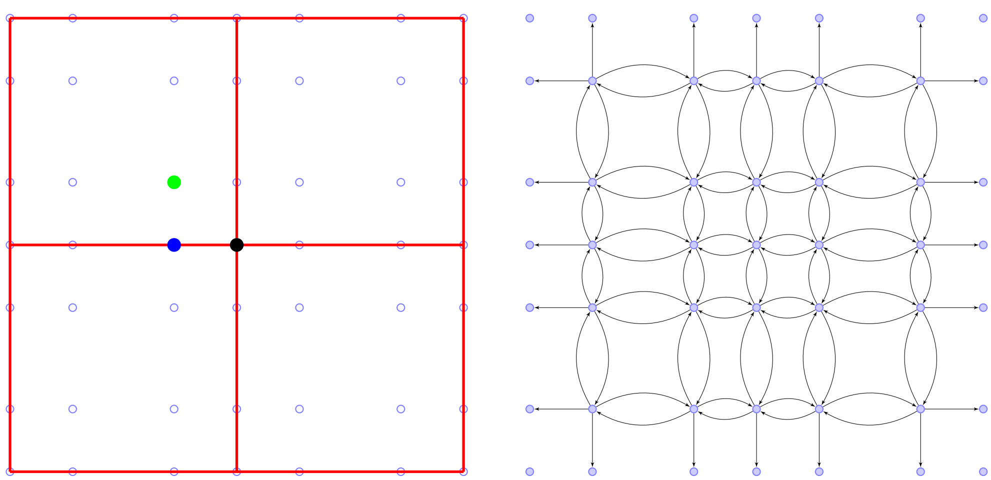

(a) Three point types defining the stencil: knot (black), edge point (blue), interior point (green).

(b) The directed graph defined by the matrix M_1.

FIG. 10. *An illustration of a Q^3 mesh with 2×2 cells.*

6.2. Two-dimensional case. Due to symmetry, the stencil of the scheme can be defined at three different types of points, see Figure 10 (a). Let each rectangular cell have size $h \times h$ and denote Q^3 scheme by $\bar{L}_h \bar{\mathbf{u}} = \bar{\mathbf{f}}$. Let $A = \frac{h^2}{4} \bar{L}_h$. Then for a boundary point $(x_i, y_j) \in \partial\Omega$, $\mathcal{A}(\bar{\mathbf{u}})_{ij} = \frac{h^2}{4} u_{ij}$. And the stencil of $\mathcal{A}$ at interior grid points is given as

$$
\textbf{$\mathcal{A}$ at knot:}\quad
\begin{array}{ccccccc}
 & & & -\frac{1}{4} & & & \\
 & & & \frac{15\sqrt{5}-25}{8} & & & \\
 & & & \frac{-15\sqrt{5}-25}{8} & & & \\
-\frac{1}{4} & \frac{15\sqrt{5}-25}{8} & \frac{-15\sqrt{5}-25}{8} & \mathbf{26} & \frac{-15\sqrt{5}-25}{8} & \frac{15\sqrt{5}-25}{8} & -\frac{1}{4} \\
 & & & \frac{-15\sqrt{5}-25}{8} & & & \\
 & & & \frac{15\sqrt{5}-25}{8} & & & \\
 & & & -\frac{1}{4} & & &
\end{array}
$$

$$
\textbf{$\mathcal{A}$ at edge point:}\quad
\begin{array}{cccc}
 & & -\frac{1}{4} & \\
 & & \frac{15\sqrt{5}-25}{8} & \\
 & & \frac{-15\sqrt{5}-25}{8} & \\
\frac{3\sqrt{5}-5}{4} & -\frac{5}{2} & \mathbf{18} & \frac{-3\sqrt{5}-5}{4} \\
 & & \frac{-15\sqrt{5}-25}{8} & \\
 & & \frac{15\sqrt{5}-25}{8} & \\
 & & -\frac{1}{4} &
\end{array}
\qquad
\textbf{$\mathcal{A}$ at interior point:}\quad
\begin{array}{cccc}
 & & \frac{3\sqrt{5}-5}{4} & \\
 & & -\frac{5}{2} & \\
\frac{3\sqrt{5}-5}{4} & -\frac{5}{2} & \mathbf{10} & \frac{-3\sqrt{5}-5}{4} \\
 & & \frac{-3\sqrt{5}-5}{4} &
\end{array}
$$

Next we list the definition of matrices A_i and Z_i by the corresponding linear operators $\mathcal{A}_i$ and $\mathcal{Z}_i$. For convenience, we will only list the stencil at interior grid points. For the domain boundary points $(x_i, y_j) \in \partial\Omega$, all A_i matrices will have the same value as A: $\mathcal{A}_i(\bar{\mathbf{u}})_{ij} = \frac{h^2}{4}u_{ij}$. And $\mathcal{Z}_i(\bar{\mathbf{u}})_{ij} = 0$ for $(x_i, y_j) \in \partial\Omega$. The matrix L_i is defined as $L_i = I + (A_i)_d^{-1} Z_i, \quad i = 0, 1, 2$. The matrices and their products are given by:

$$
\textbf{$\mathcal{A}_1$ at knot:}\quad
\begin{array}{ccccccc}
 & & & 0 & & & \\
 & & & \frac{15\sqrt{5}-25}{8} & & & \\
 & & & \frac{-15\sqrt{5}-25}{8} & & & \\
0 & \frac{15\sqrt{5}-25}{8} & \frac{-15\sqrt{5}-25}{8} & \mathbf{26} & \frac{-15\sqrt{5}-25}{8} & \frac{15\sqrt{5}-25}{8} & 0 \\
 & & & \frac{-15\sqrt{5}-25}{8} & & & \\
 & & & \frac{15\sqrt{5}-25}{8} & & & \\
 & & & 0 & & &
\end{array}
$$

$$
\textbf{$\mathcal{A}_1$ at edge point:}\quad
\begin{array}{cccc}
 & & 0 & \\
 & & 0 & \\
 & & -7 & \\
0 & -\frac{5}{2} & \mathbf{17} & -\frac{1}{100} \\
 & & -7 & \\
 & & 0 & \\
 & & 0 &
\end{array}
\qquad
\textbf{$\mathcal{A}_1$ at interior point:}\quad
\begin{array}{cccc}
 & & 0 & \\
 & & -\frac{1}{2} & \\
0 & -\frac{1}{2} & \mathbf{10} & -\frac{1}{2} \\
 & & -\frac{1}{2} &
\end{array}
$$

$$\mathcal{A}_0 \textbf{ at knot: } \begin{array}{ccccccc} & & & 0 & & & \\ & & & 0 & & & \\ & & & \frac{-15\sqrt{5}-25}{8} & & & \\ 0 & 0 & \frac{-15\sqrt{5}-25}{8} & \mathbf{30} & \frac{-15\sqrt{5}-25}{8} & 0 & 0 \\ & & & \frac{-15\sqrt{5}-25}{8} & & & \\ & & & 0 & & & \\ & & & 0 & & & \end{array}$$

$$\mathcal{A}_0 \textbf{ at edge point: } \begin{array}{cccc} & & 0 & \\ & & 0 & \\ & & -7 & \\ 0 & -\frac{1}{100} & \mathbf{17} & -\frac{1}{100} \\ & & -7 & \\ & & 0 & \\ & & 0 & \end{array} \qquad \mathcal{A}_0 \textbf{ at interior point: } \begin{array}{cccc} & & 0 & \\ & & -\frac{1}{2} & \\ 0 & -\frac{1}{2} & \mathbf{10} & -\frac{1}{2} \\ & & -\frac{1}{2} & \end{array}$$

$$\mathcal{Z}_0 \textbf{ at knot : } \begin{array}{ccccccc} & & & 0 & & & \\ & & & 0 & & & \\ & & & 0 & & & \\ 0 & 0 & 0 & \mathbf{0} & 0 & 0 & 0 \\ & & & 0 & & & \\ & & & 0 & & & \\ & & & 0 & & & \end{array}$$

$$\mathcal{Z}_0 \textbf{ at edge point: } \begin{array}{cccc} & & 0 & \\ & & 0 & \\ & & 0 & \\ 0 & -\frac{5}{2}+\frac{1}{100} & \mathbf{0} & 0 \\ & & 0 & \\ & & 0 & \\ & & 0 & \end{array} \qquad \mathcal{Z}_0 \textbf{ at interior point: } \begin{array}{cccc} & & 0 & \\ & & 0 & \\ 0 & 0 & \mathbf{0} & 0 \\ & & 0 & \end{array}$$

$$\mathcal{A}_0\mathcal{L}_0 \textbf{ at knot: } \begin{array}{ccccccc} & & & 0 & & & \\ & & & \frac{747\sqrt{5}+1245}{2720} & & & \\ & & & \frac{-15\sqrt{5}-25}{8} & & & \\ 0 & \frac{747\sqrt{5}+1245}{2720} & \frac{-15\sqrt{5}-25}{8} & \mathbf{30} & \frac{-15\sqrt{5}-25}{8} & \frac{747\sqrt{5}+1245}{2720} & 0 \\ & & & \frac{-15\sqrt{5}-25}{8} & & & \\ & & & \frac{747\sqrt{5}+1245}{2720} & & & \\ & & & 0 & & & \end{array}$$

$$\mathcal{A}_0\mathcal{L}_0 \textbf{ at edge point: } \begin{array}{cccc} & & 0 & \\ & & 0 & \\ & & -7 & \\ 0 & -\frac{5}{2} & \mathbf{17+\frac{249}{170000}} & -\frac{1}{100} \\ & & -7 & \\ & & 0 & \\ & & 0 & \end{array} \qquad \mathcal{A}_0\mathcal{L}_0 \textbf{ at interior point: } \begin{array}{ccccc} & & 0 & & \\ & & -\frac{1}{2} & \frac{249}{3400} & \\ 0 & -\frac{1}{2} & \mathbf{10} & -\frac{1}{2} & \\ & \frac{249}{3400} & -\frac{1}{2} & & \end{array}$$

$$
\mathcal{A}_2 \textbf{ at knot: }
\begin{array}{ccccccc}
 & & & -\frac{1}{4} & & & \\
 & & & \frac{15\sqrt{5}-25}{8} & & & \\
 & & & \frac{-15\sqrt{5}-25}{8} & & & \\
-\frac{1}{4} & \frac{15\sqrt{5}-25}{8} & \frac{-15\sqrt{5}-25}{8} & \mathbf{26} & \frac{-15\sqrt{5}-25}{8} & \frac{15\sqrt{5}-25}{8} & -\frac{1}{4} \\
 & & & \frac{-15\sqrt{5}-25}{8} & & & \\
 & & & \frac{15\sqrt{5}-25}{8} & & & \\
 & & & -\frac{1}{4} & & &
\end{array}
$$

$$
\mathcal{A}_2 \textbf{ at edge point: }
\begin{array}{cccc}
 & & 0 & \\
 & & \frac{15\sqrt{5}-25}{8} & \frac{1}{4} \\
 & & -7 & \\
\frac{3\sqrt{5}-5}{4} & -\frac{5}{2} & \mathbf{17} & \frac{-3\sqrt{5}-5}{4} \\
 & & -7 & \\
 & & \frac{15\sqrt{5}-25}{8} & \frac{1}{4} \\
 & & 0 &
\end{array}
\qquad
\mathcal{A}_2 \textbf{ at interior point: }
\begin{array}{cccc}
 & & 0 & \\
 & & -\frac{5}{2} & -\frac{5}{14} \\
0 & -\frac{5}{2} & \mathbf{10} & -\frac{1}{2} \\
 & -\frac{5}{14} & -\frac{1}{2} &
\end{array}
$$

$$
\mathcal{Z}_1 \textbf{ at knot : }
\begin{array}{ccccccc}
 & & & 0 & & & \\
 & & & 0 & & & \\
 & & & 0 & & & \\
0 & 0 & 0 & \mathbf{0} & 0 & 0 & 0 \\
 & & & 0 & & & \\
 & & & 0 & & & \\
 & & & 0 & & &
\end{array}
$$

$$
\mathcal{Z}_1 \textbf{ at edge point: }
\begin{array}{cccc}
 & & 0 & \\
 & & 0 & \\
 & & 0 & \\
0 & 0 & \mathbf{0} & \frac{-3\sqrt{5}-5}{4}+\frac{1}{100} \\
 & & 0 & \\
 & & 0 & \\
 & & 0 &
\end{array}
\qquad
\mathcal{Z}_1 \textbf{ at interior point: }
\begin{array}{cccc}
 & & 0 & \\
 & & -\frac{5}{2}+\frac{1}{2} & -\frac{5}{14} \\
0 & -\frac{5}{2}+\frac{1}{2} & \mathbf{0} & 0 \\
 & -\frac{5}{14} & 0 &
\end{array}
$$

$$
\mathcal{A}_1\mathcal{L}_1 \textbf{ at knot: }
\begin{array}{ccccccc}
 & & & \frac{3\sqrt{5}-505}{2720} & & & \\
 & & & \frac{15\sqrt{5}-25}{8} & & & \\
 & & & \frac{-15\sqrt{5}-25}{8} & & & \\
\frac{3\sqrt{5}-505}{2720} & \frac{15\sqrt{5}-25}{8} & \frac{-15\sqrt{5}-25}{8} & \mathbf{26+4(\frac{747\sqrt{5}+1745}{2720})} & \frac{-15\sqrt{5}-25}{8} & \frac{15\sqrt{5}-25}{8} & \frac{3\sqrt{5}-505}{2720} \\
 & & & \frac{-15\sqrt{5}-25}{8} & & & \\
 & & & \frac{15\sqrt{5}-25}{8} & & & \\
 & & & \frac{3\sqrt{5}-505}{2720} & & &
\end{array}
$$

$$
\mathcal{A}_1\mathcal{L}_1 \textbf{ at edge point: }
\begin{array}{cccc}
 & & 0 & \\
 & & \frac{7}{5} & \frac{1}{4} \\
 & \frac{7}{5} & -7 & \\
\frac{75\sqrt{5}+124}{680} & -\frac{5}{2}+2(\frac{1}{4}) & \mathbf{17} & \frac{-3\sqrt{5}-5}{4} \\
 & \frac{7}{5} & -7 & \\
 & & \frac{7}{5} & \frac{1}{4} \\
 & & 0 &
\end{array}
\qquad
\mathcal{A}_1\mathcal{L}_1 \textbf{ interior point: }
\begin{array}{cccc}
 & \frac{1}{56} & 0 & \\
\frac{1}{56} & 2(\frac{1}{10}) & -\frac{5}{2} & -\frac{5}{14} \\
0 & -\frac{5}{2} & \mathbf{10+2(\frac{1}{10})} & -\frac{1}{2}+\frac{1}{56} \\
 & -\frac{5}{14} & -\frac{1}{2}+\frac{1}{56} & 2(\frac{75\sqrt{5}+124}{3400})
\end{array}
$$

$$\textbf{$\mathcal{Z}_2$ at knot:}\quad \begin{array}{ccccccc}
 & & & 0 & & & \\
 & & & 0 & & & \\
 & & & 0 & & & \\
0 & 0 & 0 & \mathbf{0} & 0 & 0 & 0\\
 & & & 0 & & & \\
 & & & 0 & & & \\
 & & & 0 & & &
\end{array}$$

$$\textbf{$\mathcal{Z}_2$ at edge point:}\quad \begin{array}{cccc}
 & & 0 & \\
 & & 0 & \\
 & & 0 & \\
0 & 0 & \mathbf{0} & 0\\
 & & 0 & \\
 & & 0 & \\
 & & 0 &
\end{array}
\qquad
\textbf{$\mathcal{Z}_2$ at interior point:}\quad \begin{array}{cccc}
 & & 0 & \\
 & & 0 & \\
0 & 0 & \mathbf{0} & -2\\
 & & -2 &
\end{array}$$

$$\textbf{$\mathcal{A}_2\mathcal{L}_2$ at knot :}\quad \begin{array}{ccccccc}
 & & & -\frac{1}{4} & & & \\
 & & & \frac{15\sqrt{5}-25}{8} & & & \\
 & & & \frac{-15\sqrt{5}-25}{8} & & & \\
-\frac{1}{4} & \frac{15\sqrt{5}-25}{8} & \frac{-15\sqrt{5}-25}{8} & \mathbf{26} & \frac{-15\sqrt{5}-25}{8} & \frac{15\sqrt{5}-25}{8} & -\frac{1}{4}\\
 & & & \frac{-15\sqrt{5}-25}{8} & & & \\
 & & & \frac{15\sqrt{5}-25}{8} & & & \\
 & & & -\frac{1}{4} & & &
\end{array}$$

$$\textbf{$\mathcal{A}_2\mathcal{L}_2$ at edge point:}\quad \begin{array}{cccc}
 & & \frac{-3\sqrt{5}+5}{8} & \\
 & & \frac{15\sqrt{5}-25}{8} & \frac{1}{4}+\frac{-3\sqrt{5}+5}{8}\\
 & & -7 & \frac{7}{5}\\
\frac{3\sqrt{5}-5}{4} & -\frac{5}{2} & \mathbf{17+2(\frac{7}{5})} & \frac{-3\sqrt{5}-5}{4}\\
 & & -7 & \frac{7}{5}\\
 & & \frac{15\sqrt{5}-25}{8} & \frac{1}{4}+\frac{-3\sqrt{5}+5}{8}\\
 & & \frac{-3\sqrt{5}+5}{8} &
\end{array}
\qquad
\textbf{$\mathcal{A}_2\mathcal{L}_2$ at interior point:}\quad \begin{array}{cccc}
 & 0 & \frac{1}{2} & \\
0 & 0 & -\frac{5}{2} & -\frac{5}{14}+\frac{1}{2}\\
\frac{1}{2} & -\frac{5}{2} & \mathbf{10} & -2-\frac{1}{2}\\
 & -\frac{5}{14}+\frac{1}{2} & -2-\frac{1}{2} & 0
\end{array}$$

By Theorem 2.1, A_0 is an M-matrix, thus we set $M_1 = A_0$. Notice that the matrix $M_1 = A_0$ has a 5-point stencil and the directed graph defined by M_1 is given in Figure 10 (b), in which there is a directed path starting from any interior grid point to any other point. For convenience, let $A_3 = A$. Then we have $\mathcal{A}_k(\mathbf{1}) \geq 0$ $(k = 0, 1, 2, 3)$. Moreover, $\mathcal{A}_k(\mathbf{1})_{ij} > 0$ $(k = 0, 1, 2, 3)$ for domain boundary point $(x_i, y_j) \in \partial\Omega$. The directed graph defined by M_1 easily implies that M_1 connects $\mathcal{N}^0(A_i\mathbf{1})$ with $\mathcal{N}^+(A_i\mathbf{1})$ for all $i = 0, 1, 2, 3$.

By straightforward comparison, we can verify that $A_1 \leq A_0L_0, A_2 \leq A_1L_1, A \leq A_2L_2$. By Theorem 4.3, we have

$$A_1 \leq A_0L_0 = M_1L_0 \Rightarrow A_1 = M_1M_2 \Rightarrow A_2 \leq M_1M_2L_1 \Rightarrow A_2 = M_1M_2M_3$$

$$\Rightarrow A \leq M_1M_2M_3L_2 \Rightarrow A = M_1M_2M_3M_4 \Rightarrow A^{-1} \geq 0.$$

7. Numerical Tests.

7.1. Efficient implementation. For all schemes discussed in this paper, except the P^2 variational difference scheme, the stiffness matrix can be efficiently inverted by an eigenvector method, very similar to the inversion of 5-point discrete Laplacian by Fast Fourier Transform (FFT). We demonstrate it for the 9-point scheme on a $N_x \times N_y$ grid. For instance, the stiffness matrix in the scheme (2.2) can be written as

$$-\frac{1}{6h^2}[H_x \otimes H_y - 36 I_x \otimes I_y],$$

where $\otimes$ is the Kronecker product, I_x is the identity matrix of size $N_x \times N_x$ and H_x and H_y are symmetric tridiagonal matricies of size $N_x \times N_x$ and $N_y \times N_y$ respectively, with H defined as

$$H = \begin{pmatrix} 4 & 1 & & & & \\ 1 & 4 & 1 & & & \\ & 1 & 4 & 1 & & \\ & & \ddots & \ddots & \ddots & \\ & & & 1 & 4 & 1 \\ & & & & 1 & 4 \end{pmatrix}.$$

Let $H = S\Lambda S^{-1}$ be the eigenvalue decomposition of H, then we also have the eigenvalue decomposition of stiffness matrix

$$-\frac{1}{6h^2}[H_x \otimes H_y - 36 I_x \otimes I_y] = -\frac{1}{6h^2}(S_x \otimes S_y)(\Lambda_x \otimes \Lambda_y - 36 I_x \otimes I_y)(S_x^{-1} \otimes S_y^{-1}).$$

Therefore, the stiffness matrix can be efficiently inverted by the eigenvector method, e.g., Section 7.4 in [19]. Moreover, for a matrix H of size $n \times n$, its m-th eigenvector is $\begin{bmatrix}\sin(m\pi\frac{1}{n+1}) & \cdots & \sin(m\pi\frac{n}{n+1})\end{bmatrix}^T$ and corresponding eigenvalue is $4+2\cos(m\pi\frac{1}{n+1})$. Thus multiplication of S and S^{-1} can be implemented through FFT.

The stiffness matrix in the Q^k variational difference scheme also has a kron structure [19]. But such a kron structure does not seem possible for (3.4). For Q^2/Q^3 and Bramble-Hubbard schemes, the eigenvectors for the small matrices H_x and H_y can be computed numerically.

7.2. Accuracy tests. We show some accuracy tests of the schemes mentioned in this paper for solving $-\Delta u = f$ on a square $(0,1) \times (0,1)$ with Dirichlet boundary conditions. Quasi-uniform meshes were generated by setting each pair of consecutive finite element cells along the axis to have a fixed ratio $\frac{h_k}{h_{k-1}} = 1.01$. We will simply refer to the classical 9-point scheme (2.1) as 9-point scheme, and refer to its variant (2.3) as compact finite difference. The schemes are tested for the following very smooth solutions:

1. The Laplace equation $-\Delta u = 0$ with Dirichlet boundary conditions and $u(x,y) = log((x+1)^2 + (y+1)^2) + sin(y)e^x$.
2. Poisson equation $-\Delta u = f$ with homogeneous Dirichlet boundary condition:
$$\begin{aligned} f(x,y) &= 13\pi^2 sin(3\pi y)sin(2\pi x) + 2y(1-y) + 2x(1-x) \\ u(x,y) &= sin(3\pi y)sin(2\pi x) + xy(1-x)(1-y) \end{aligned} \tag{7.1}$$
3. Poisson equation $-\Delta u = f$ with nonhomogeneous Dirichlet boundary condition:
$$\begin{aligned} f &= 74\pi^2 cos(5\pi x)cos(7\pi y) - 8 \\ u &= cos(5\pi x)cos(7\pi y) + x^2 + y^2 \end{aligned} \tag{7.2}$$

The errors of fourth order accurate schemes on uniform grids are listed in Table 1, Table 2 and Table 3. The errors of Q^2 and P^2 variational difference scheme on quasi uniform rectangular meshes are listed in Table 4. The errors of Q^3 variational difference scheme on uniform rectangular meshes are listed in Table 5. For the Laplace equation, 9-point scheme (2.1) and compact finite difference (2.3) are the same scheme and they are indeed sixth order accurate, see Remark 1.

TABLE 1
Accuracy test on uniform meshes for $-\Delta u = 0$.

Finite Difference Grid	Q^2 variational difference				P^2 variational difference				9-point scheme (2.1)			
	l^2 error	order	l^∞ error	order	l^2 error	order	l^∞ error	order	l^2 error	order	l^∞ error	order
7×7	1.04E-5	-	2.50E-5	-	2.05E-5	-	3.89E-5	-	1.50E-9	-	3.52E-9	-
15×15	6.91E-7	3.92	1.81E-6	3.78	1.38E-6	3.89	2.83E-6	3.78	2.35E-11	5.99	5.51E-11	6.00
31×31	4.42E-08	3.96	1.26E-7	3.83	8.93E-08	3.95	2.05E-7	3.78	3.98E-13	5.88	8.89E-13	5.95
63×63	2.79E-9	3.98	8.56E-9	3.88	5.65E-9	3.98	1.41E-8	3.85	1.32E-13	1.58	2.37E-13	1.90

Finite Difference Grid	compact finite difference (2.3)				Bramble-Hubbard scheme			
	l^2 error	order	l^∞ error	order	l^2 error	order	l^∞ error	order
7×7	1.50E-9	-	3.52E-9	-	5.04E-5	-	6.97E-5	-
15×15	2.35E-11	5.99	5.51E-11	6.00	3.75E-6	3.74	5.34E-06	3.70
31×31	3.98E-13	5.88	8.89E-13	5.95	2.52E-7	3.89	3.86E-7	3.78
63×63	1.32E-13	1.58	2.37E-13	1.90	1.63E-08	3.95	2.77E-8	3.80

TABLE 2
Accuracy test on uniform meshes for (7.1).

Finite Difference Grid	Q^2 variational difference				P^2 variational difference				9-point scheme (2.1)			
	l^2 error	order	l^∞ error	order	l^2 error	order	l^∞ error	order	l^2 error	order	l^∞ error	order
7×7	2.22e-02	-	4.90e-02	-	4.50e-02	-	1.67e-01	-	2.22e-04	-	4.45e-04	-
15×15	1.31e-03	4.08	3.03e-03	4.01	2.49e-03	4.17	9.42e-03	4.15	5.63e-06	5.30	1.12e-05	5.30
31×31	8.04e-05	4.02	1.88e-04	4.01	1.50e-04	4.05	5.69e-04	4.04	2.32e-07	4.59	4.65e-07	4.59
63×63	5.00e-06	4.00	1.17e-05	4.00	9.30e-06	4.01	3.52e-05	4.01	1.27e-08	4.19	2.54e-08	4.19

Finite Difference Grid	compact finite difference (2.3)				Bramble-Hubbard scheme			
	l^2 error	order	l^∞ error	order	l^2 error	order	l^∞ error	order
7×7	3.18E-3	-	6.36E-3	-	3.74E-2	-	8.62E-2	-
15×15	1.91E-4	4.05	3.82E-4	4.05	2.36E-3	3.98	5.28E-3	4.02
31×31	1.18E-5	4.01	2.36E-5	4.01	1.01E-4	4.54	2.11E-4	4.64
63×63	7.38E-7	4.00	1.47E-6	4.00	4.17E-6	4.60	7.89E-6	4.74

TABLE 3
Accuracy test on uniform meshes for (7.2).

Finite Difference Grid	Q^2 variational difference				P^2 variational difference				9-point scheme (2.1)			
	l^2 error	order	l^∞ error	order	l^2 error	order	l^∞ error	order	l^2 error	order	l^∞ error	order
7×7	3.62E-1	-	1.10E-0	-	9.68E-1	-	2.59E-0	-	2.48E-2	-	5.69E-2	-
15×15	3.75E-2	3.26	9.68E-2	3.50	7.81E-2	3.63	3.00E-1	3.11	2.61E-4	6.56	6.46E-4	6.45
31×31	2.44E-3	3.94	7.18E-3	3.75	4.70E-3	4.05	1.84E-2	4.02	3.65E-5	2.84	8.97E-5	2.85
63×63	1.54E-4	3.98	5.50E-4	3.70	2.89E-4	4.02	1.11E-3	4.04	2.55E-6	3.83	6.57E-6	3.77

Finite Difference Grid	compact finite difference (2.3)				Bramble-Hubbard scheme			
	l^2 error	order	l^∞ error	order	l^2 error	order	l^∞ error	order
7×7	9.88E-2	-	2.26E-1	-	3.14E-1	-	8.23E-1	-
15×15	5.40E-3	4.19	1.33E-2	4.08	1.76E-2	4.15	6.16E-2	3.73
31×31	3.22E-4	4.06	7.91E-4	4.07	3.38E-3	2.37	1.15E-2	2.41
63×63	1.98E-5	4.01	5.11E-5	3.95	3.04E-4	3.47	1.20E-3	3.32

8. Concluding remarks. We reviewed four existing high order monotone discrete Laplacian. By verifying a relaxed Lorenz's condition, we have discussed suitable mesh constraints, under which the fourth order accurate Q^2 variational difference on quasi-uniform meshes is monotone. The fifth order accurate Q^3 variational difference scheme on a uniform mesh is proven be a product of four M-matrices thus inverse positive.

TABLE 4
Accuracy test on quasi-uniform meshes.

Finite Difference Grid	Ratio $\frac{h_i}{h_{i-1}}$	Q^2 variational difference		P^2 variational difference	
		l^∞ error	order	l^∞ error	order
test on $-\Delta u = 0$					
7×7	1.01	2.66E-5	-	3.98E-5	-
15×15	1.01	1.97E-6	3.74	3.17E-6	3.65
31×31	1.01	1.54E-7	3.67	2.57E-7	3.62
63×63	1.01	1.37E-8	3.49	2.74E-8	3.22
test on (7.1)					
7×7	1.01	4.92E-2	-	1.69E-1	-
15×15	1.01	3.19E-3	3.94	9.90E-3	4.10
31×31	1.01	2.29E-4	3.79	6.72E-4	3.87
63×63	1.01	1.80E-5	3.67	5.34E-5	3.65
test on (7.2)					
7×7	1.01	1.20E-0	-	2.95E-0	-
15×15	1.01	1.03E-1	3.54	3.56E-1	3.05
31×31	1.01	9.10E-3	3.50	2.48E-2	3.84
63×63	1.01	9.64E-4	3.23	1.80E-3	3.77

TABLE 5
Accuracy test of Q^3 variational difference scheme on uniform meshes.

Q^3 Finite Element Mesh	Finite Difference Grid	l^2 error	order	l^∞ error	order
test on $-\Delta u = f$					
2×2	5×5	1.89E-4	-	4.71E-4	-
4×4	11×11	6.88E-8	4.78	2.46E-7	4.26
8×8	23×23	2.23E-9	4.88	9.90E-9	4.64
16×16	47×47	7.61E-11	4.94	3.98E-10	4.64
32×32	95×95	2.44E-12	4.96	1.41E-11	4.82
test on (7.1)					
2×2	5×5	3.28E-2	-	5.53E-2	-
4×4	11×11	1.58E-3	4.38	3.51E-3	3.98
8×8	23×23	4.81E-5	5.03	1.13E-4	4.96
16×16	47×47	1.48E-6	5.03	3.52E-6	5.00
test on (7.2)					
2×2	5×5	1.18E0	-	2.61E0	-
4×4	11×11	6.08E-2	4.28	1.45E-1	4.17
8×8	23×23	2.87E-3	4.40	7.10E-3	4.35
16×16	47×47	9.82E-5	4.87	2.41E-4	4.88
32×32	95×95	3.12E-6	4.97	7.60E-6	4.99

REFERENCES

[1] E. Bohl and J. Lorenz, *Inverse monotonicity and difference schemes of higher order. a summary for two-point boundary value problems*, aequationes mathematicae, 19 (1979), pp. 1–36.

[2] J. Bramble and B. Hubbard, *On the formulation of finite difference analogues of the Dirichlet problem for Poisson's equation*, Numerische Mathematik, 4 (1962), pp. 313–327.

[3] J. Bramble and B. Hubbard, *On a finite difference analogue of an elliptic boundary problem which is neither diagonally dominant nor of non-negative type*, Journal of Mathematics and Physics, 43 (1964), pp. 117–132.

[4] J. H. Bramble, *Fourth-order finite difference analogues of the Dirichlet problem for Poisson's equation in three and four dimensions*, Mathematics of Computation, 17 (1963), pp. 217–222.

[5] J. H. Bramble and B. E. Hubbard, *New monotone type approximations for elliptic problems*, Mathematics of Computation, 18 (1964), pp. 349–367.

[6] C. Chen, *Structure theory of superconvergence of finite elements (In Chinese)*, Hunan Science and Technology Press, Changsha, 2001.

[7] I. Christie and C. Hall, *The maximum principle for bilinear elements*, International Journal for Numerical Methods in Engineering, 20 (1984), pp. 549–553.

[8] P. G. Ciarlet, *Discrete maximum principle for finite-difference operators*, Aequationes mathematicae, 4 (1970), pp. 338–352.

[9] P. G. Ciarlet, *The Finite Element Method for Elliptic Problems*, Society for Industrial and Applied Mathematics, 2002.

[10] L. Collatz, *The numerical treatment of differential equations*, Springer-Verlag, Berlin, 1960.

[11] B. Fornberg and N. Flyer, *A primer on radial basis functions with applications to the geosciences*, SIAM, 2015.

[12] L. Fox, *Some improvements in the use of relaxation methods for the solution of ordinary and partial differential equations*, Proceedings of the Royal Society of London. Series A. Mathematical and Physical Sciences, 190 (1947), pp. 31–59.

[13] W. Höhn and H. D. Mittelmann, *Some remarks on the discrete maximum-principle for finite elements of higher order*, Computing, 27 (1981), pp. 145–154.

[14] Y. Huang and J. Xu, *Superconvergence of quadratic finite elements on mildly structured grids*, Mathematics of computation, 77 (2008), pp. 1253–1268.

[15] V. I. Krylov and L. V. Kantorovitch, *Approximate methods of higher analysis*, P. Noordhoff, 1958.

[16] S. K. Lele, *Compact finite difference schemes with spectral-like resolution*, Journal of computational physics, 103 (1992), pp. 16–42.

[17] H. Li, S. Xie, and X. Zhang, *A high order accurate bound-preserving compact finite difference scheme for scalar convection diffusion equations*, SIAM Journal on Numerical Analysis, 56 (2018), pp. 3308–3345.

[18] H. Li and X. Zhang, *On the monotonicity and discrete maximum principle of the finite difference implementation of C^0-Q^2 finite element method*, Numerische Mathematik, (2020), pp. 1–36.

[19] H. Li and X. Zhang, *Superconvergence of high order finite difference schemes based on variational formulation for elliptic equations*, Journal of Scientific Computing, 82 (2020), p. 36.

[20] J. Lorenz, *Zur inversmonotonie diskreter probleme*, Numerische Mathematik, 27 (1977), pp. 227–238.

[21] R. J. Plemmons, *M-matrix characterizations. I—-nonsingular M-matrices*, Linear Algebra and its Applications, 18 (1977), pp. 175–188.

[22] T. Vejchodskỳ and P. Šolín, *Discrete maximum principle for higher-order finite elements in 1D*, Mathematics of Computation, 76 (2007), pp. 1833–1846.

[23] L. Wahlbin, *Superconvergence in Galerkin finite element methods*, Springer, 2006.

[24] J. Whiteman, *Lagrangian finite element and finite difference methods for poisson problems*, in Numerische Behandlung von Differentialgleichungen, Springer, 1975, pp. 331–355.

[25] J. Xu and L. Zikatanov, *A monotone finite element scheme for convection-diffusion equations*, Mathematics of Computation of the American Mathematical Society, 68 (1999), pp. 1429–1446.